





## Article

# The Pretare-Piedilama Clastic Deposit: New Evidence of a Quaternary Rock Avalanche Event in Central Apennines (Italy)

Maria Luisa Putignano<sup>1</sup>, Emiliano Di Luzio<sup>1,\*</sup>, Luca Schilirò<sup>1</sup>, Andrea Pietrosante<sup>1</sup>  
and Salvatore Ivo Giano<sup>2</sup>

<sup>1</sup> CNR-IGAG, Consiglio Nazionale delle Ricerche, Istituto di Geologia Ambientale e Geoingegneria, Montelibretti, Via Salaria km 29.3, Monterodondo St., 00165 Rome, Italy

<sup>2</sup> Department of Sciences, University of Basilicata, Campus Macchia Romana, Via Ateneo Lucano 10, 85100 Potenza, Italy

\* Correspondence: emiliano.diluzio@igag.cnr.it

**Abstract:** This paper deals with the origin of the Pretare clastic deposit (PRA), which crops out along the Morriconne fluvial valley in the Central Apennines of Italy. With the aim of deciphering the genesis of the PRA deposit, geological s.l. and geomorphological analyses were carried out allowing for the interpretation of the PRA deposit as a rock avalanche. Furthermore, geological cross sections constrained by well-log and field survey data, together with stratigraphic, sedimentologic, and morphometric analyses, allowed us to assign the deposit to a catastrophic rock slope failure, which occurred during a cold climate of the Late Pleistocene. Several issues concerning the propagation mechanisms were inferred from the mapping of 350 boulders over the entire accumulation area and from the measure of the morphometric parameters of the landslide body. We also performed a restoration of the potential source area by comparing the reconstructed pre- and post-failure DEMs. A missing volume of  $8.41 \times 10^6 \text{ m}^3$  was estimated on the south-eastern side of the Vettore Mt., which is consistent with the deposit volume computed from the geological interpretation ( $10.56 \times 10^6 \text{ m}^3$ ). The outcomes of this study provide useful insights for a better understanding of the Quaternary morpho-evolution of the Central Apennines area where analogous rock avalanche events marked the recent evolution of the belt.



**Citation:** Putignano, M.L.; Di Luzio, E.; Schilirò, L.; Pietrosante, A.; Giano, S.I. The Pretare-Piedilama Clastic Deposit: New Evidence of a Quaternary Rock Avalanche Event in Central Apennines (Italy). *Water* **2023**, *15*, 753. <https://doi.org/10.3390/w15040753>

Academic Editor: Peiyue Li

Received: 26 January 2023

Revised: 9 February 2023

Accepted: 11 February 2023

Published: 14 February 2023



**Copyright:** © 2023 by the authors. Licensee MDPI, Basel, Switzerland. This article is an open access article distributed under the terms and conditions of the Creative Commons Attribution (CC BY) license (<https://creativecommons.org/licenses/by/4.0/>).

**Keywords:** rock avalanche; morphometric analysis; Late Pleistocene; Central Apennines; Italy

## 1. Introduction

Rock avalanches are extremely rapid mass movements of fragmented rocks, deriving from large rock slope failures [1–3]. These phenomena occur in many parts of the world and often testify to the recent Quaternary morphological evolution of mountain belts [4–8]. In this respect, different authors [9–16] have suggested that rock avalanches can represent the short-term evolution of Deep-seated Gravitational Slope Deformations (DGSDs). In Italy, this type of catastrophic rock slope failure has been well documented in some historical Alpine case histories, such as the Vajont [17,18] and the Val Pola landslides [19,20].

In the Central Apennines, and in particularly in the central sector of the mountain belt, in the last three decades several rock avalanche deposits, Middle Pleistocene to Holocene in age, were identified within intermontane basins and/or narrow valleys [13,14,21–27]. These deposits have been interpreted as resulting from rock avalanche events according to a variety of specific outcrop-scale features, as observed in similar worldwide case-histories such as: (i) heterogeneous grain size distribution, with the prevalence of sandy matrix, resulting from the fragmentation of the collapsed material [28]; (ii) low morphometric evolution of rock blocks [13,29–31]; (iii) the presence of localized carapace facies overlaying the internal debris and consisting of less-fragmented, coarser blocks [32,33]; (iv) pseudo-fluidal structures as thrust-like surfaces [24,34,35]; and (v) preservation of unbroken stratigraphic sections within the fragmented deposit with both normal or reverse polarity [24,36–38].

The accumulation areas of rock avalanche deposits, in a single mountain slope, usually feature a long run-out [2,39–44] due to shattering and expanding mechanisms that coupled with air or mechanical fluidization to produce a flow-like motion of fragmented rocks [45]. These areas can also exhibit remarkable run-up zones related to the high velocity reached by the flowing of materials [2,24,25,45–49], and often present a hummocky topography [36,37,50–52] with steep frontal and distal ridges. Finally, a gradual change of clast size depending on the distance from the source area was also recognized [53–55]. In addition to these general observations, the geomorphological context of the central Apennines produced singular characteristics [13]. In many cases, the reduced width of the intramontane valleys or the presence of incised paleo-valleys prevented the radial spreading of rock avalanches. Post-depositional erosion processes tended to obliterate the original morphology of the accumulation area, beveling the frontal and lateral edges. Finally, the presence of different types of clastic deposits at the base of mountain ridges (e.g., tectonic breccias, debris avalanches, debris flows, glacial deposits, etc.) may lead to misinterpretation of the sediment origin due to their similarity with the rock avalanche deposits.

Given these statements, this study describes the results of a multidisciplinary analysis aimed to characterize a large Quaternary clastic deposit observed in the eastern piedmont junction area of Mt. Vettore (2476 m a.s.l.), which shows features typical of rock avalanches. The study area borders the Sibillini Range (Figure 1), along which the tectonic juxtaposition of Mesozoic slope-to-basin carbonates over Miocene flysch deposits occurred during the Mio-Pliocene tectonogenesis of the belt [56,57]. The same region has been affected by Quaternary tectonic activity [58] and was involved in the 2016–2017 seismic sequence that occurred in Central Italy [56–61].

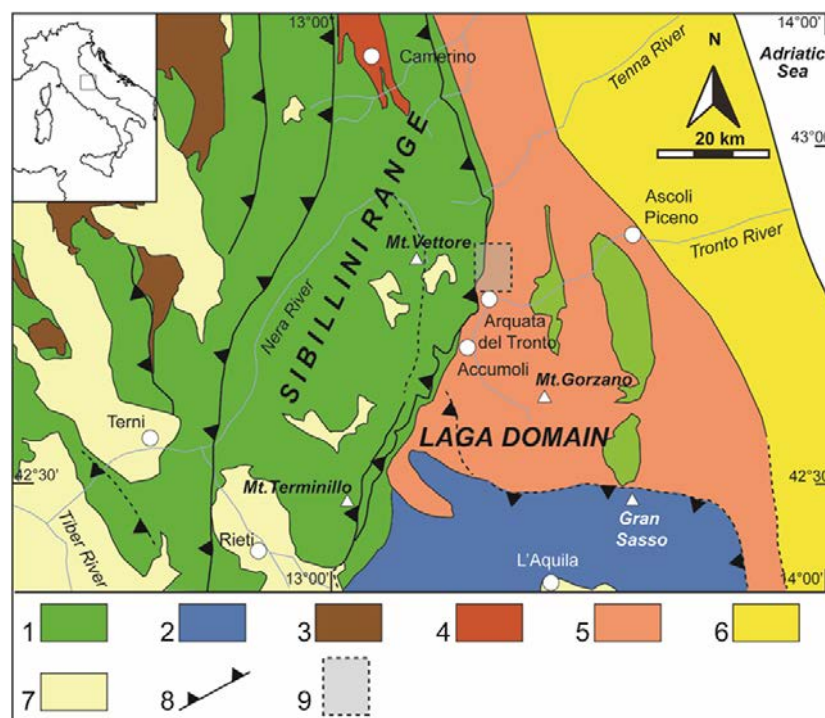


**Figure 1.** Geological sketch map of the study area (after [57]). Legend: 1. Calcareous, marly-calcareous and marly basin sequences of the Umbria-Marche-Sabina Apennines (Upper Trias—Miocene p.p.); 2. Calcareous and marly-calcareous platform-slope sequence of the Latium-Abruzzi Apennines (Upper Trias—Miocene p.p.); 3. Miocene siliciclastic turbiditic deposits (Burdigalian p.p.—Tortonian p.p.); 4. Miocene siliciclastic deposits (Serravallian p.p.—Messinian p.p.); 5. Miocene siliciclastic deposits for the Laga sequence (Messinian p.p.); 6. Pliocene to Pleistocene marine and continental peri-Adriatic deposits; 7. Post-orogenic marine and continental deposits (Pliocene to Quaternary); 8. Main thrust front; 9. Study area.

The clastic deposit crops out within the Morricono Stream valley (Figure 2A) and are composed of huge calcareous blocks with sharp edges and sandy-gravel matrix-supported, partly hidden by shrub-like vegetation or buildings (Figure 2B,C). Detailed geological and geomorphological field investigations were completed, together with sedimentological, stratigraphical, and morphometric analyses of the clastic deposits, with the aim of supporting the hypothesis of a rock avalanche event, unlike the previous interpretation of the debris-flow deposit that was proposed [58]. The estimation of the debris volume was also performed through the results of well-log analysis. The volume estimation of clastic deposits was compared to the rock volume missing from two box-shaped detachment areas which were identified on the south-eastern slope of the Sibillini Range, in the Aia della Regina area (Figure 2A). Well-log analysis [62] also demonstrated the presence, at different depths, of several landslide deposits between the rock avalanche deposition and the geological bedrock of the Laga Formation [63–65], thus testifying to the persistent condition of slope instabilities in the area during the Quaternary. The depositional process of the rock avalanche deposits were inferred from the main textural and morphometric characteristics of the clastic deposits, and were then related to the geological factors controlling the Quaternary morpho-evolution of the area, such as the erosive processes and tectonics. The Pretare-Piedilama rock avalanche can be considered from this perspective, similar to other huge rock slope failures of the Central Apennine as a formative event with persistent geomorphic effects on the local environment. Its investigation has been useful in the improvement of the surface dynamics knowledge that occurred in a very resilient landscape such as those of the Vettore mountain area.

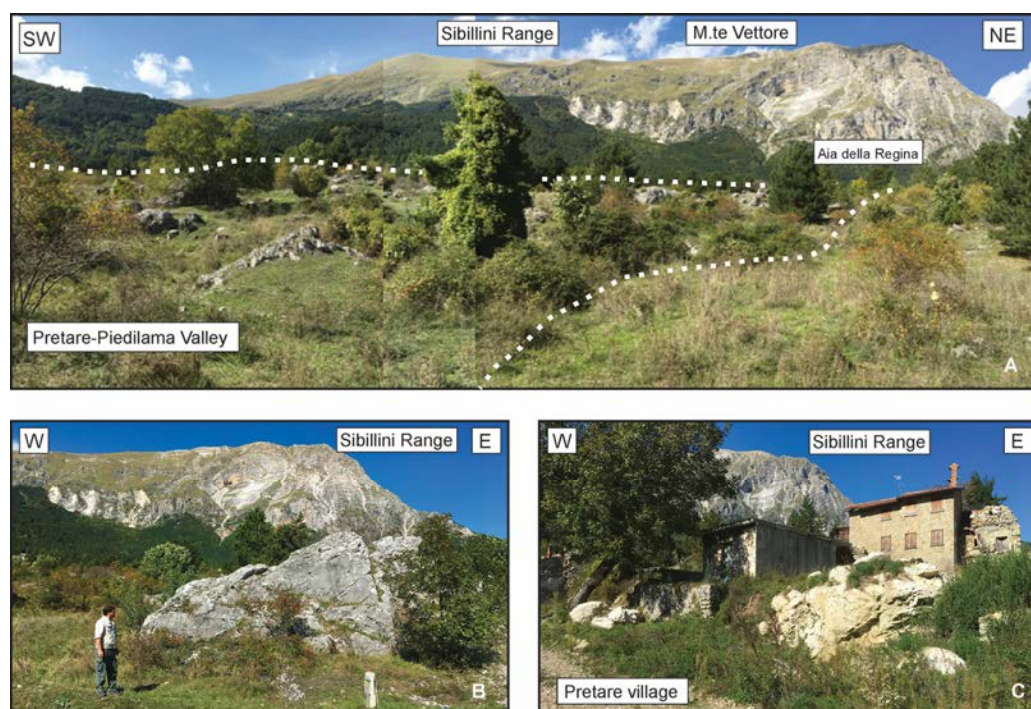


**Figure 2.** (A) panoramic view of the clastic deposits filling the Pretare-Piedilama Valley, and the Sibillini Range in the background; (B) huge, sharp rock block lying in the mid-sector of the valley; (C) rock blocks of the Pretare village.

## 2. Materials and Methods

Geological surveys were carried out at a 1:10,000 scale, producing a detailed geological map. The field analyses were integrated by data coming from the scientific literature [66] and by new stratigraphic and sedimentological data furnished by boreholes crossing the entire Quaternary succession down to the Miocene bedrock. Details were provided by Quaternary clastic deposits with the purpose of obtaining the relative timing of the main

depositional/erosional events occurring in that area. Furthermore, a geomorphological mapping of relic and recent structural and fluvial landforms was carried out, thus furnishing the past and present modelling processes acting on the landscape.

The analysis and characterization of the Pretare clastic deposit, the field surveys, the sedimentological-textural analyses and the morphometric/geometric investigations of both deposit and potential source area were performed. Considering the wide grain size range featuring the deposits (from plurimetric-sized boulders to gravelly-sandy matrix), the analyses were conducted at two different scales. For boulders and blocks we prepared a specific database in a GIS environment by mapping the position, measuring the observable dimensions, and estimating the volume of each rock block over the entire depositional area. For the matrix, we collected six samples that were representative of different sectors of the deposit. Following the standard procedure of ASTM D422-63 for particle-size analysis [67], we collected 5 kg of material for each sample due to the poor assortment of the deposit. The grain size analysis was performed only for material retained at the sieve n.200 (0.075 mm) which was passed, after exsiccation, through a pile of sieves stacked in a mechanical shaker.

With regard to the morphometric analysis of the potential source area, a comparison between the present-day DEM and the reconstructed original one (i.e., before the rock detachment and failure event) was carried out. Specifically, we used the “thin plate technique” [68,69] in a GIS environment for interpolating contour lines. First, we interpolated the present day contour lines which, in turn, were rectified for the restoration of the presumed, original topography. As a result, we obtained two different 2m-resolution DEMs representative of the current topography and of the original one. The pre-failure and post-failure DEM surfaces were then compared in order to estimate the rock-avalanche volume immediately after the detachment.

### 3. Geological and Geomorphological Settings

The study area is located in the Umbria-Marche Apennines, a north-east and east-verging fold-and-thrust belt generated by the convergence of collisional margins of the European and African plates during the Mesozoic and Cenozoic eras [70]. Neogene contractional structures are represented in the study area by N-S-striking thrusts, which involved the eastern sector of the Sibillini Ridge. Here, above an upper Triassic-lower Jurassic carbonate platform sequence (Calcare Massiccio Fm.) lies Jurassic to Cretaceous deep-water carbonate units related to the Umbria-Marche basin domain. The carbonate units were tectonically juxtaposed, from the Messinian times until to the Pliocene [71,72], on the turbidite units of the Laga Fm. (Figures 1 and 3), which were deposited in the Messinian foredeep [73,74]. The basal thrust is the northern edge of a regional feature known as the “Olevano-Antrodoco-Monti Sibillini line” [72] that corresponds to the tectonic boundary between the Central and the Northern Apennines [56]. In the study area, the “Olevano-Antrodoco-Monti Sibillini” thrust is an oblique ramp with an N-S trend and a right-lateral kinematics [72,75–78]. In the footwall of the Sibillini thrust front, the siliciclastic Laga sequence is deformed in an N-S oriented thrust-and-fold belt with wide overturned sectors, including the Acquasante Terme and Montagna dei Fiori culmination zones (Figures 1 and 3).

Starting from the Lower Pleistocene, a new geodynamic regime with a NE-SW-striking extensional axis took place [1] or [79,80] and was responsible, in some cases, for the re-activation of normal faults of the older compressive structures (negative tectonic inversion). However, an extension was accommodated along the NW-SE and WNW-ESE-oriented normal faults that have controlled the Quaternary continental deposition within tectonically-related intramontane basins [81]. Active faults are found in this portion of the central Apennines, such as the Gorzano and Vettore faults (Figure 3), responsible for the 2016 earthquake [82].

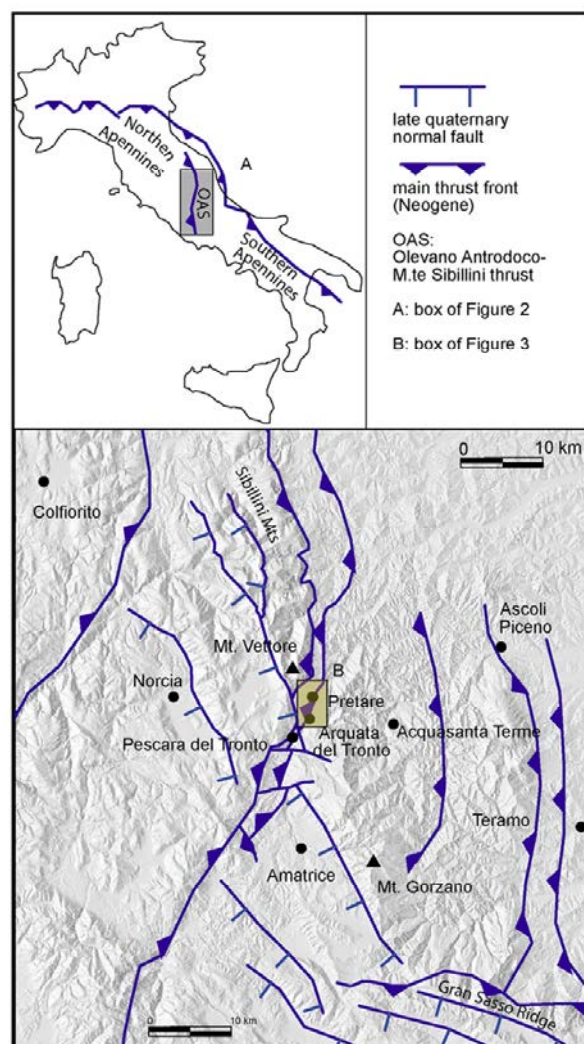


**Figure 3.** Structural sketch map of the axial zone of the Central-Northern Apennines chain showing the NE–SW-oriented normal fault segments and the main thrust lines.

From a geomorphological point of view, the Pretare-Piedilama area is included in a narrow NNE–SSW-oriented catchment fluvial basin of about 12.5 km<sup>2</sup> in width. The drainage basin shows an asymmetric drainage net with the main and most developed stream channels flowing from NW to SE on the right-side valley as tributaries of the Morricone-Pianella stream valley, forming a trellis-like pattern. The Morricone-Pianella stream is a left tributary of the Tronto River forming at its mouth a narrow and entrenched valley of about 1 km-length which was filled by several orders of unpaired fluvial terraces. The confluence of the Morricone-Pianella Stream in the Tronto River corresponds to a large local base level which represents the morphological threshold of the Pleistocene Amatrice intermontane basin [83]. The threshold of that basin is also suggested by two main morphological features. The first is a knickpoint occurring in the Tronto longitudinal channel profile and placed at about 580–600 m of elevation a.s.l., and the second is a strong change of channel flow direction in the Tronto River. These morphological features represent the morphological response of the Tronto river valley to the regional tectonic uplift which affected the whole Amatrice basin and surroundings, suggesting a steady state configuration in the upstream reach of the Tronto River [84]. Indeed, the fault system activity seems to have inhibited the backward fluvial wave incision which started in the palaeo Tronto River mouth ~450 ky because of the Middle Pleistocene uplift ([84] and references therein).

## 4. Results

### 4.1. Local Geomorphology

The main morphostructural features of the studied area are the Vettore and Vettoreto Mts representing the main mountain peaks which bend westward and reach an elevation of 2476 and 2055 m a.s.l., respectively. They form an N-S-oriented asymmetrical fold with a gently dipping western limb and a vertical to overturned eastern limb [54]. In the study area, the tectonic overthrusting of the carbonate successions on the turbiditic sequence and the later, Quaternary faulting led to the formation of the Vettore-Vettoreto obsequent thrust-fault scarp landform (numbered 1 in the legend of Figure 4). This structural landform is the wider among the geomorphological features of the Pretare-Piedilama area, reaching about 5 km in length. The transient state of that obsequent scarp was the principal inheritance cause of the slope deposits' abundance produced during cold stages in Quaternary times. The footwall slope of the overthrust anticline shows several minor folding structures in the Laga Fm, which results in N-S-oriented anticline ridges and syncline valleys.

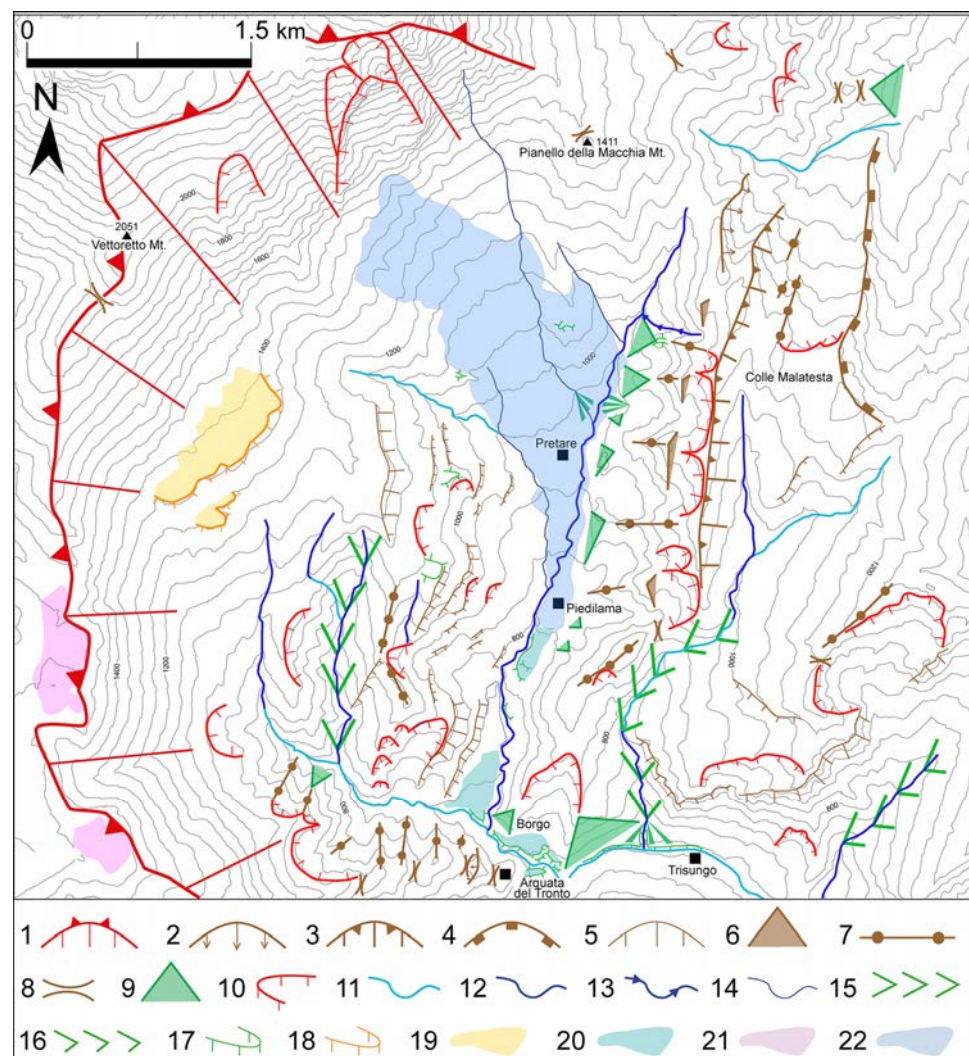


**Figure 4.** Geomorphological sketch map of the study area. Legend: (1) obsequent fault slope; (2) structurally-controlled slope; (3) hogback; (4) homoclinal ridge; (5) litho-structural scarp; (6) flat iron; (7) straight ridge; (8) saddle; (9) triangular facets; (10) degradational and/or landslide scarp; (11) transverse stream; (12) strike stream; (13) anti-dip stream; (14) consequent stream; (15) V-shaped valley; (16) asymmetric valley; (17) fluvial terrace scarp; (18) glacis scarp; (19) fluvial terrace tread; (20) glacis surface; (21) erosional surface; (22) Pretare rock avalanche area.

The most evident NE-SW and NNE-SSW-oriented structural landforms are distributed both in the left and right sides of the Fosso Morricone and Fosso della Pianella stream valleys (Figure 5). In the right-side of that latter valley, there are several litho-structural scarps formed into low-erodible rocks. Structural-controlled slopes such as hogback and homoclinal ridges are significantly exposed in the study area. Remnants of ancient erosion surfaces (number 21 in Figure 4) sculptured during the warm climate episodes of a Pliocene marine transgression event [81,85] are found on the top of the Vettore and Vettoretto Mts. They are polygenic landforms with a gentle-dipping or a flat surface that was firstly modelled by marine processes [85], and secondly re-shaped by subaerial processes during Pliocene-Pleistocene times [81,85,86]. The drainage network shows a trellis-like pattern and the main channels flow from the northeast to the southwest. The two main streams of Fosso Morricone-Fosso della Pianella and Fosso La valle are left-tributaries of the Tronto River. They flow in a NNE-SSW-oriented synclinal fold structure forming strike streams. The streams, close to Pretare and Piedilama villages, flow within V-shaped or asymmetric valleys features. Minor streams flowing from NW to SE are placed in the right-side valley of the Fosso Morricone-Fosso della Pianella Stream. In that place there are consequent streams and transverse streams (Figure 4). The latter streams transversally cut the NNE-SSW-oriented folding structures formed in the arenaceous successions and contribute to sculpture flat irons, strike ridge divides, and triangular facets landforms (Figure 4).

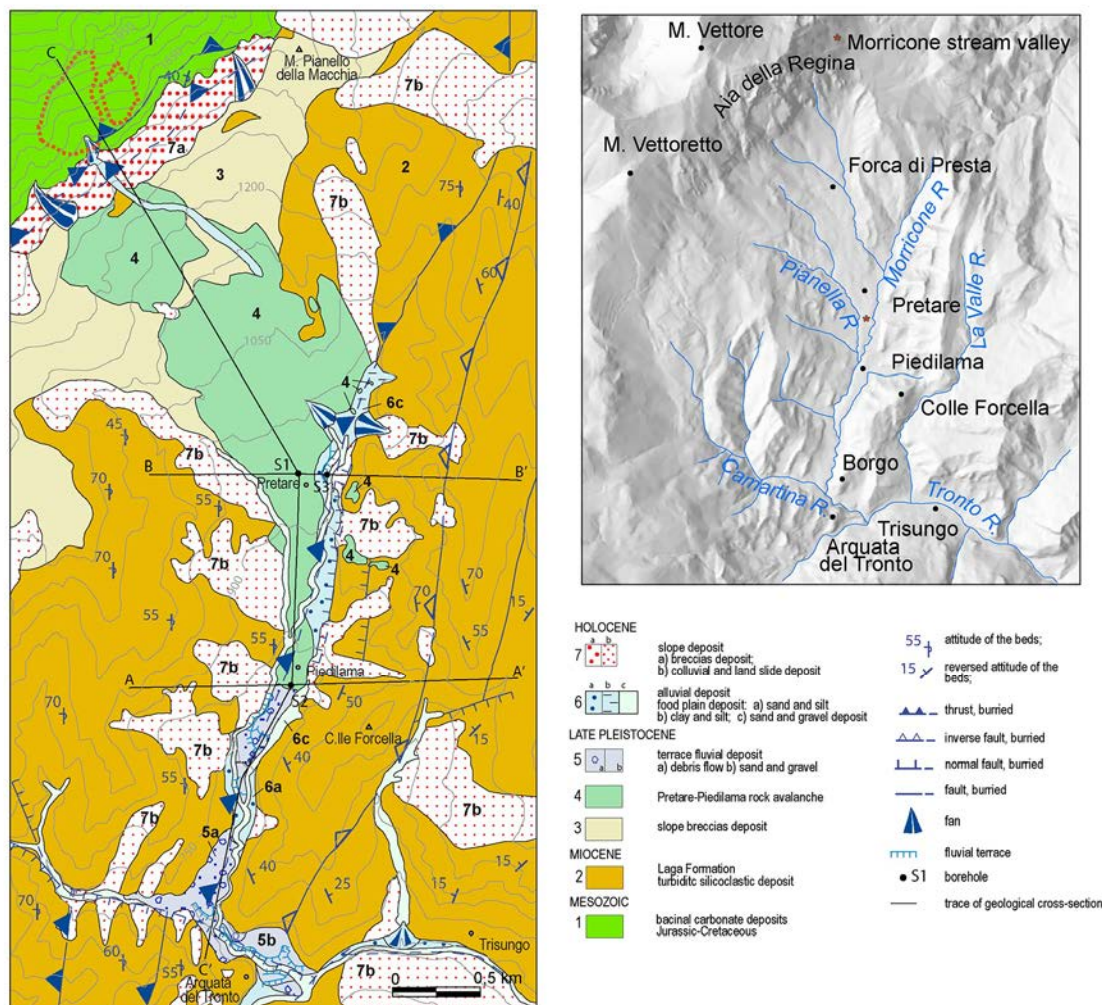


**Figure 5.** Geological sketch map of the investigated area realized by a 1:10.000 scale field survey (for location see the box in Figure 2); the contour line interval is 75 m. Hillshade of the study area including the main drainage network.

#### 4.2. Local Geology

The investigated area included the basal portion of relief of Mt. Vettore (Aia della Regina to Arquata del Tronto village and is crossed by the Morricone stream valley, a fluvial incision extending in a N-S direction from Pretare-Piedilama villages up to Arquata del Tronto village (Figure 5). New geological field surveys of 1:10.000 scale were carried out in the last years in the frame of the new Geological Sheet 337 “Norcia” of the CARG Project of Italy.

The main tectonic feature is characterized by the Mt Sibillini thrust (unit 1) overlapping the Laga Fm (unit 2). Minor compressive feature is the N-S-oriented thrust intersecting the Laga Fm (unit 2). The bedrock geometry favored the vertical incision of narrow and long streams such as the Morricone and Pianella streams that flow south to the village of Arquata del Tronto, where they merge into the Tronto River (Figure 5).

The Quaternary deposits are largely distributed along the whole western side of the Morricone Stream valley, also reaching the piedmont sector of the Mt. Vettore carbonate slope. Here, Late Pleistocene talus slope deposits (unit 3) composed of stratified, clast-supported breccias have been found. Holocene era younger talus deposits (unit 6d) rest on the previous ones thus form the upper junction with the carbonate bedrock. Both the Holocene and the Late Pleistocene slope deposits were involved in mass movements, thus producing landslides and debris flow deposits (unit 6e).

The deposit of rock avalanches (unit 4) crops out at the base of the carbonate slope of Mt Vettore and is hosted in the Morricone stream valley, between the Piedilama and Pretare villages. That deposit was the object of deeper multidisciplinary analyses illustrated in the next sections. The rock avalanches' deposit seems to be attributable to a large rock fall composed of heterometric calcareous blocks of 1 m<sup>3</sup> to 10 m<sup>3</sup> in size, with a sandy-gravelly matrix. In the lower reach of the Morricone Stream valley a more recent fluvial deposit crops out and was terraced by a progressive vertical incision of the Morricone Stream (unit 5). The oldest deposit (unit 5a) is a torrential fluvial succession, mainly generated by a re-working of unit 4. It was formed by massive and matrix-supported calcareous gravels with a sandy-silty matrix and is about 20–30 m thick with poor- to well-rounded clasts. Unit 5a rests on the rock avalanche deposit and is distributed from the Piedilama village to the Borgo village (Figure 5). Close to the Borgo village, up to the confluence to the Tronto River, there are other fluvial terraced deposits (unit 5). Both the units 5a and 5b form several fluvial terraces placed at different elevations and ranging from 800 to 675 m a.s.l. The fluvial terrace deposits are formed by the last two units (4 e 5) and are both tentatively attributed to the Late Pleistocene era according to [55]. In the central reach of the Morricone Stream valley are found Holocene deposits representing slope deposit (unit 6c) and the floodplain deposit (unit 6a,b), These deposits host the village of both the Pretare and Piedilama. Overall, these deposits unconformably cover the deposits of the unit 4.

Three boreholes have been drilled in the floodplain of the Morricone Stream (Figure 5). The S1 e S2 revealed a maximum thickness of about 74 m of Quaternary gravel and sandy-gravel debris slope deposits and finer fluvial deposits resting on the Miocene bedrock of the Laga Fm (unit 2). In particular, the borehole core showed that the Pretare-Piedilama fluvial valley was primarily filled with clastic deposits produced by subaerial denudation processes which acted both on the carbonate rocks of the Sibillini Ridge and on the arenaceous rocks of the Laga Fm, and subordinately on alluvial deposits. The clastic sediments include four detrital depositional episodes, separated by thin and sometimes weathered silty-clayey levels that pertained to a fluvial plain (L) (Figure 6). A gravel and sand fluvial succession (AL in Figure 6) has been recognized at the bottom of the S2 (15 m thickness), which tapers rapidly towards the north, reaching a minimum thickness of 3.5 m in the S1.

The sequence I, II, and III are characterized by debris slope deposits composed of carbonate and sandstone clasts (more than 1 m of diameter) with an abundant silty and sandy matrix.





on the analysis, we can consider about 22 m to be the maximum thickness of the unit 4 (S2) in the lower middle portion of the valley. This last sequence corresponds to unit 4 in Figure 6. Sequence III is related to unit 3 in Figure 6. The age of the sequences I and II, and that of the basal alluvial sediments are tentatively assigned to the Early Late Pleistocene based on the geological and geomorphological chronological attribution of morphological features by Cacciuni et al., (1995) and Aringoli et al., (2021) [81,83], and the deposits by Tortorici et al., (2009) [58].

Three geological sections are made up for the correlation of the clastic deposition (Figure 7). Along the section about N-S (C-C' in Figure 5), it is possible to reconstruct the entire Quaternary filling sequence of the Morricone stream valley that is carved within the Messinian deposits of the Laga Fm. A wedge-shaped body with a maximum thickness of about 74 m in unit 4 covers the sandstone substrate and reaches a thickness of about 40 m (section A-A' in Figure 7).

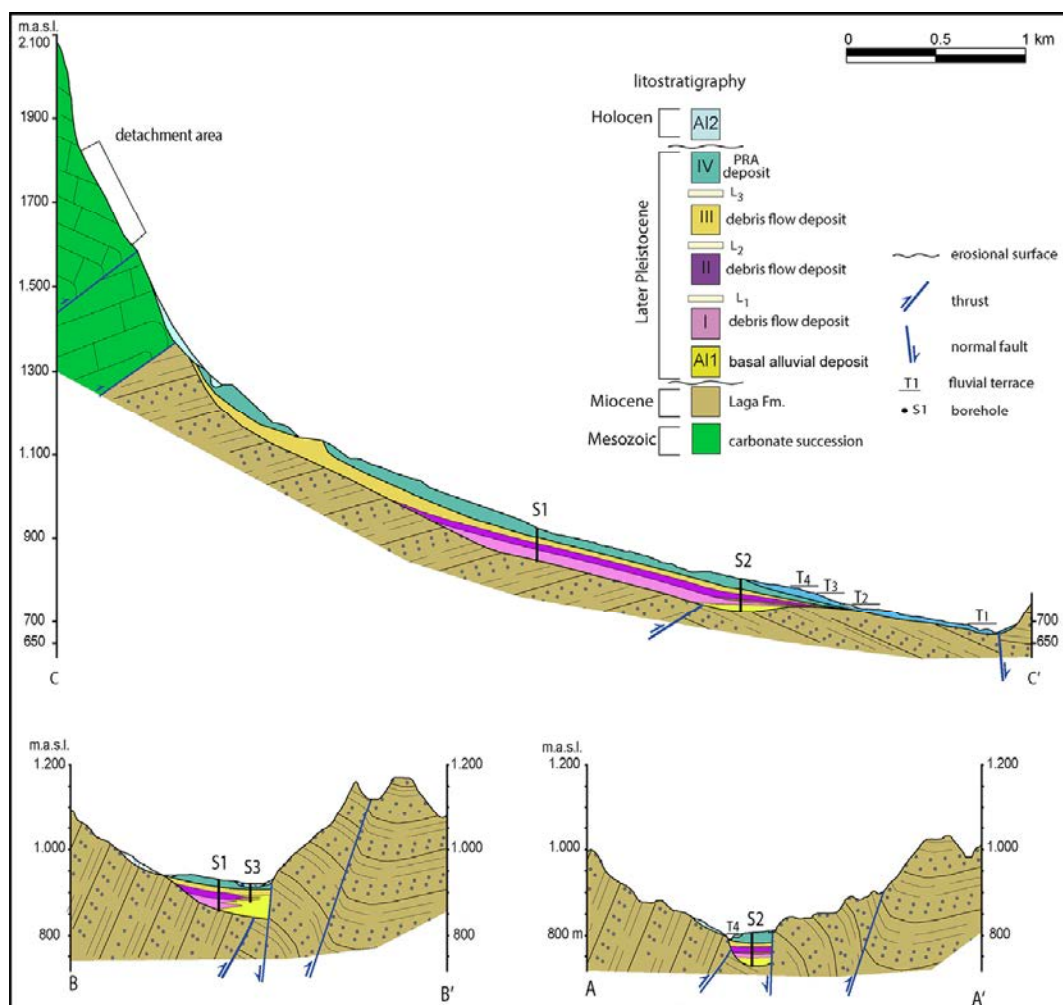


**Figure 7.** Geological cross sections cutting the S1, S2, and S3 boreholes.

The depositional episodes recognized from the boreholes interpretation are only located in the central and lower part of the Morricone valley. Section E-W (A-A' and B-B' in Figure 5) highlights the rapid lateral closure of the sedimentary body inside the valley. This morphology is inherited by the morphostructural set-up. Basal alluvial events (S1, S2) demonstrate that the beginning of the sedimentation was marked by the presence of the Morricone Stream palaeo-bed.

### 4.3. The Pretare-Piedilama Rock Avalanche

#### 4.3.1. General Features

Detailed geological relief was made in the Pretare-Piedilama rock avalanche (PRA in this text) which corresponds with unit 4 in Figure 5. In the uppermost zone, the deposit shows a NW-SE elongation, and along its western edge, rock debris are superimposed on the unit 3 slope deposits. On the eastern bound they directly cover the LAG Fm (unit 2) bedrock. Both the middle and lower zones are N-S elongated and bounded by the LAG bedrock on both sides of the narrow Morricone stream valley.

In the northern sector of the study area, the erosive stratigraphic boundary between the PRA deposit and the unit 3 slope detritus (Figure 8A) can be observed. Moreover, north to the same place, the erosive boundary between of the PRA deposit and the LAG bedrock is shown; the rock debris fill a palaeovalley bounded by erosional surfaces sculptured in arenaceous beds, at about 1050 m of elevation a.s.l. (Figure 8B). Regional geomorphological correlation allowed us to assign to Middle Pleistocene the terraced surfaces [81,83] representing a *post-quem* relative dating of the rock avalanche.

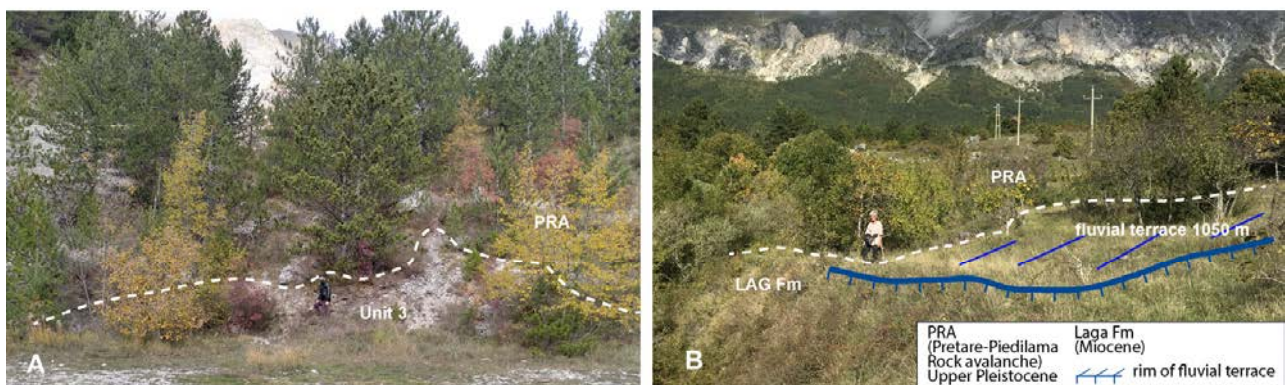


**Figure 8.** (A) Details of the erosional bound between the PRA deposit (Pretare-Piedilama rock avalanche) and the unit 3 (slope detritus) northern to the Pretare village. (B) Panoramic view of the contact between the PRA deposit remnants and the LAG bedrock. The PRA deposits rest on a terraced erosional surface placed at about 1050 m of elevation a.s.l.

In the northern slope of the Pretare village, the PRA deposits rest both on the Laga bedrock (Figure 9), and on the debris deposit of the unit 4 (Figure 10). The PRA deposit filling the middle-lower Morricone stream valley is also distributed east of the Pretare village where isolated remnants rest on the Laga bedrock. Both the bedrock and the superposed PRA deposit were affected by N-S-oriented normal faults, suggesting a recent faulting activity of the area, as already proposed by Tortorici et al. (2009) [58] (Figure 5). The latter activity is also observed through a partial run up of the rock avalanche deposits. Isolated blocks of PRA are found within the Holocene floodplain of the upper sector of the Morricone stream valley.

#### 4.3.2. Sedimentological and Textural Features

The Pretare-Piedilama deposit includes rock blocks of largely variable size that can be found in clusters within a finer matrix or as isolated features. In the first case, the main size varies from a few decimetres to approximately one to two meters (Figure 10A), while in the second case the dimensions may be even greater than 10 m (Figure 10B). The clasts' shape, which is dominantly angular to sub-angular, indicates a low textural maturity which, in turn, is consistent with the transport and depositional mechanisms of a high-energy, dry granular flow. The deposit structure is generally chaotic, but it can locally show the typical "carapace" facies with coarser blocks placed above a finer debris (Figure 10C). Samples taken from the matrix (Figure 11A) show a sandy-gravel texture with a minimal amount of silt and clay (Figure 11B) [28,55]. The sand proportion is higher in the two samples

collected just outside the southern limit of the landslide body (i.e., 1, 2 in Figure 11A,B), within a colluvial deposit resulting from the reworking of the frontal ridge material.

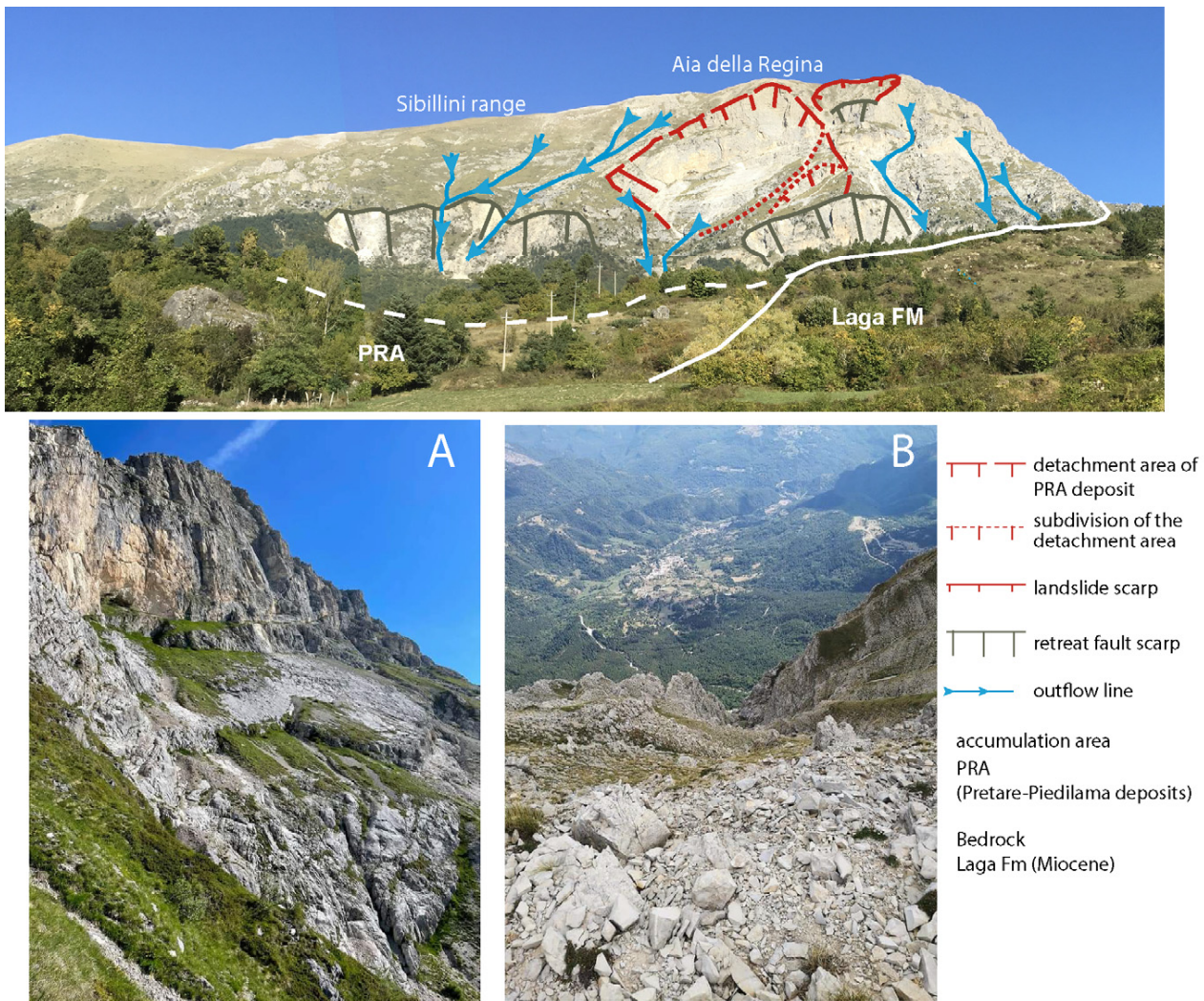


**Figure 9.** Panoramic view of the Monte Vettore fault scarp, of the detachment area of the rock avalanche, and of the contact between PRA deposit (Pretare-Piedilama rock avalanche) and the Laga Fm. (A) detail of the detachment area at the Aia della Regina, (B) erosive outflow channel flowing in the lower part of the detachment area.

The lithology of blocks mainly pertains to the Lower Jurassic carbonate facies cropping out in the Sibillini Mountain Range, i.e., the shallow-water Calcare Massiccio Formation and, subordinately, the basin-derived Corniola Formation [57]. The first one can be recognized by its massive structure (Figure 12a) in the southern sectors of the accumulation area, while the second one, which is generally well-stratified (10–50 cm thick beds), has been mainly observed in the northern sectors of the landslide body (Figure 12b).

In the Pretare village, we recognized a narrow band of clastic deposits showing a mud-supported grainstone texture (Figure 12c); these facies generally identify the stratigraphic boundary between the Calcare Massiccio and Corniola formations in the Sibillini Range [57]. Thus, even if it is not possible to draw a clear stratigraphic boundary given the large number of blocks scattered on the ground, the accumulation area (Figure 12e) seems to maintain the original slope stratigraphy with a normal polarity (Figure 12e).

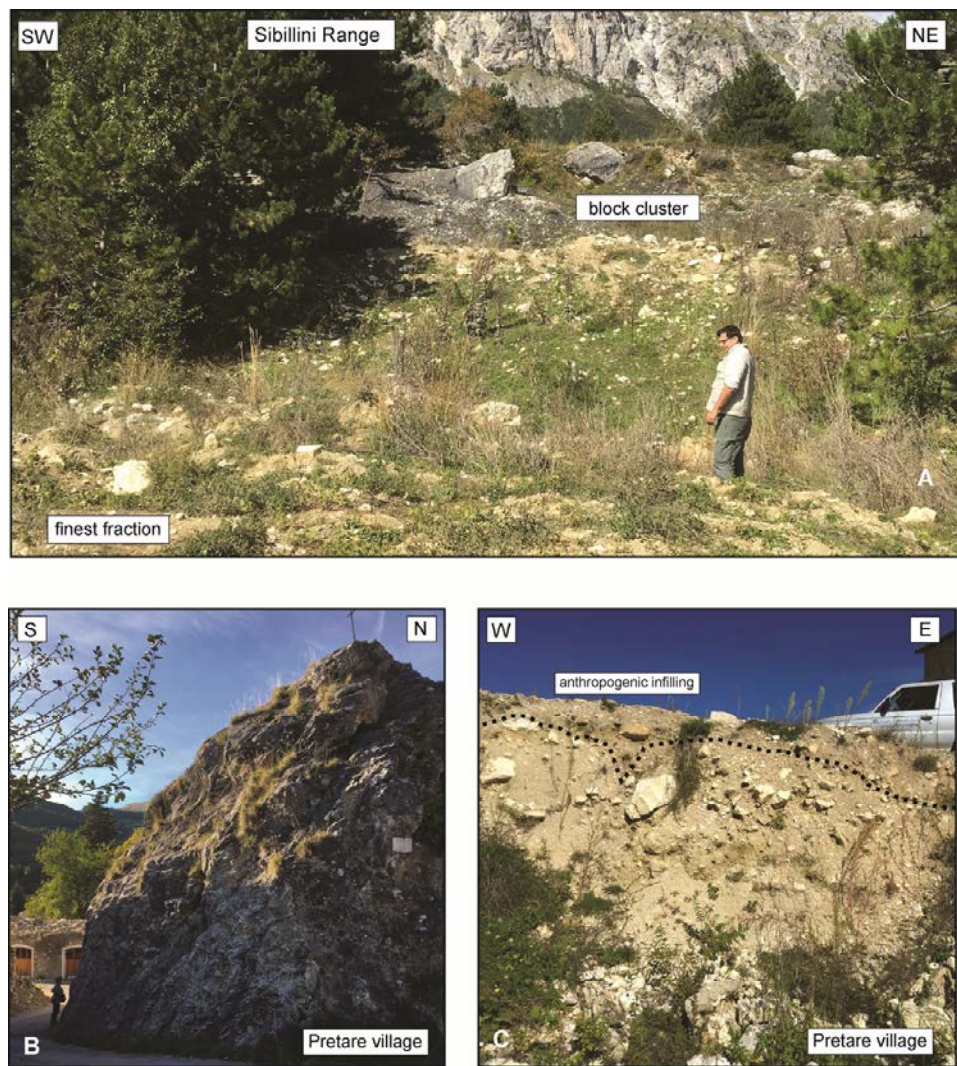


**Figure 10.** (A) Matrix-supported facies of the Pretare-Piedilama clastic deposits; (B) example of isolated mega-block; (C) carapace facies overlaying debris deposit.

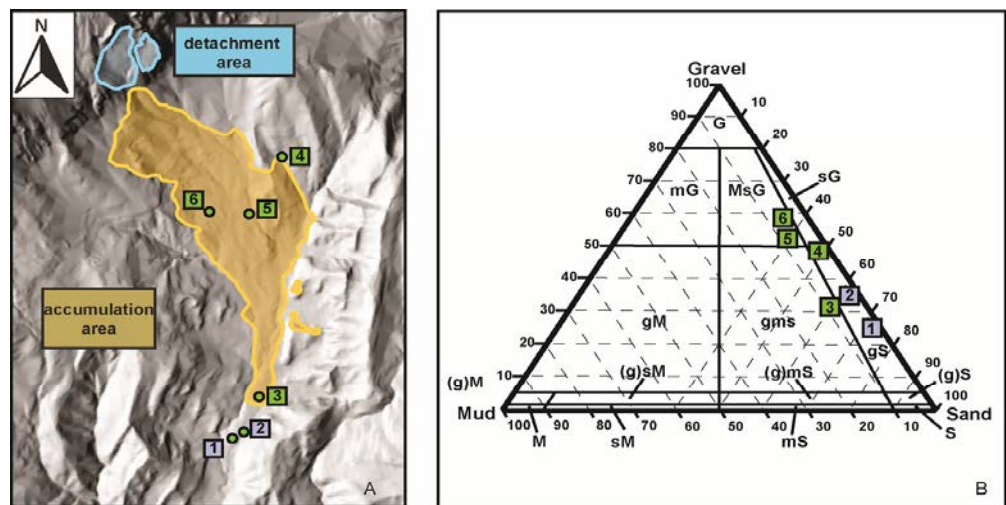


**Figure 11.** (A) location of sampling sites within (3–6) and outside (1–2) the landslide’s accumulation area; (B) particle-size texture of the matrix according to Folk’s (1980) classification.

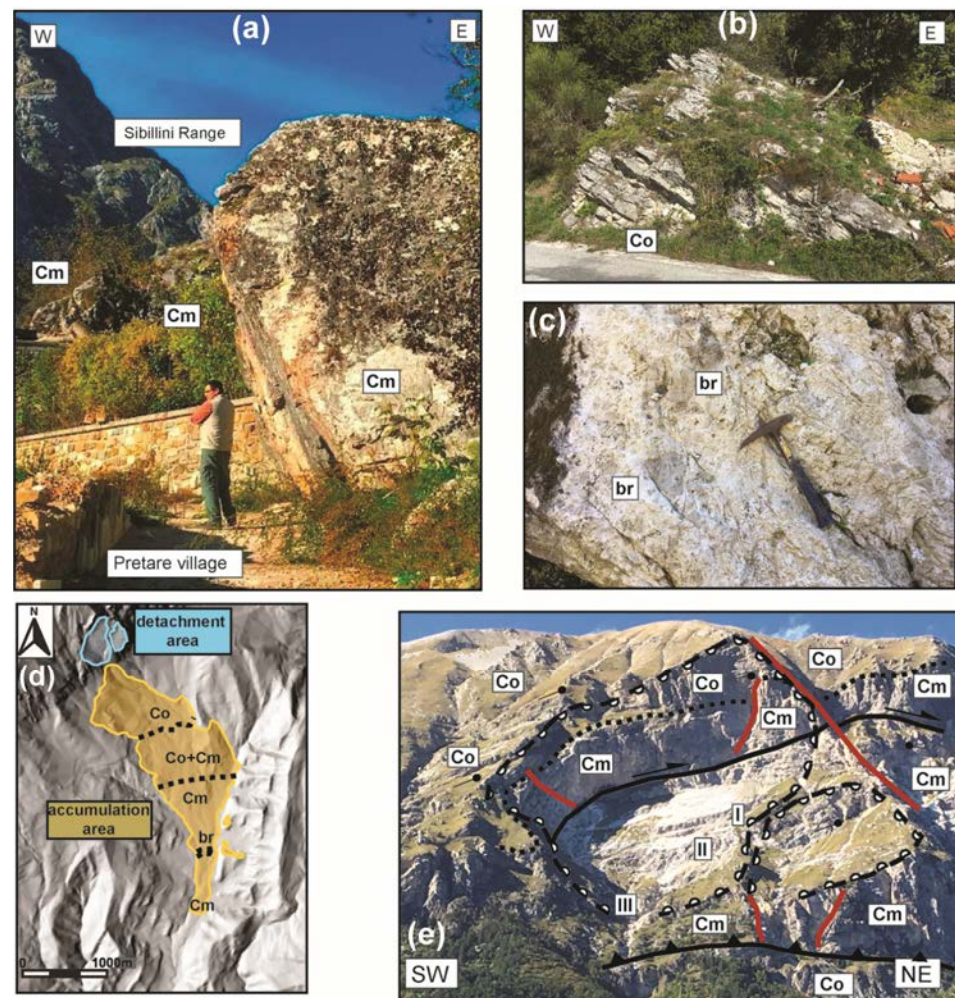


**Figure 12.** Distribution of lithologies: (a) massive calcareous blocks from the Calcare Massiccio Fm.; (b) thin bedding featuring the Corniola Fm. blocks; (c) breccia texture in a block found in the Pretare village; (d) boundaries between blocks with different lithology in the accumulation area and detachment area; (e) slope stratigraphy and main morphological features; legend: br = breccia facies; Cm = Calcare Massiccio Fm; Co = Corniola Fm; I–III morphological steps on the main sliding surface.

As regards the volume of isolated blocks, we directly measured the dimensions of 350 boulders distributed in 68 survey stations. The volumes of a single block are extremely variable (from few  $\text{dm}^3$  to almost  $1000 \text{ m}^3$ ) although rarely exceeding  $6 \text{ m}^3$  (Table 1). Starting from field data, we then inferred the maximum ( $V_{\text{max}}$ ) and average ( $V_{\text{mean}}$ ) volume of each cluster block. Significant differences may result between these two parameters, especially in the stations where the number of blocks is high (e.g., station n. 49). The  $V_{\text{max}}$  distribution map (Figure 13A) shows that the largest boulders are mostly concentrated along the middle ranges of the proximal and central sectors of the accumulation area. Moving down, the huge slope blocks ( $>100 \text{ m}^3$ ) did not overcome the Pretare village and surroundings. The same effect, although less pronounced, can be seen on the  $V_{\text{mean}}$  distribution map (Figure 13B). The smallest blocks in the  $V_{\text{max}}$  map can be found both along the middle range of the accumulation area (stations 42, 43, 46, 50 in Figure 13A) and along the lateral ridges (stations 6, 17, 39, 60, 61); a similar distribution also features the  $V_{\text{mean}}$  map (Figure 13B). Finally, another aspect that can be pointed out is the concentration of a relatively high number of blocks of different sizes in the valley narrowing along the N–S direction, south of Pretare village (Figure 13A,B).

**Table 1.** Number, mean volume ( $V_{\text{mean}}$ ) and maximum volume ( $V_{\text{max}}$ ) of the blocks identified in each station during the field survey. In the upper part is the synthesis of the block's volume distribution.

Volume Distribution							
Total n. of blocks: 350 Minimum value: 0.03 m <sup>3</sup> 1st quartile (Q1): 1.08 m <sup>3</sup>				2nd quartile (Q2): 2.25 m <sup>3</sup> 3rd quartile (Q3): 5.34 m <sup>3</sup> Maximum value: 960 m <sup>3</sup>			
Station	n. blocks	$V_{\text{mean}}$ (m <sup>3</sup> )	$V_{\text{max}}$ (m <sup>3</sup> )	Station	n. blocks	$V_{\text{mean}}$ (m <sup>3</sup> )	$V_{\text{max}}$ (m <sup>3</sup> )
1	5	2.1	7.2	35	1	16.2	16.2
2	5	1.5	2.4	36	4	21.3	81.0
3	1	30.6	30.6	37	4	4.0	10.0
4	4	2.1	7.2	38	3	4.6	7.4
5	2	39.3	78.4	39	1	3.0	3.0
6	3	0.6	0.8	40	1	24.0	24.0
7	1	37.1	37.1	41	3	16.9	24.0
8	4	4.9	17.1	42	1	4.5	4.5
9	5	18.6	91.0	43	1	4.5	4.5
10	3	4.3	11.9	44	3	260.1	360.0
11	5	2.0	7.5	45	16	38.8	150.0
12	2	4.8	6.9	46	10	2.2	2.2
13	12	1.1	1.1	47	1	108.0	108.0
14	12	5.1	25.4	48	2	25.8	40.5
15	1	7.5	7.5	49	21	39.0	560.0
16	3	33.2	99.0	50	12	2.2	2.2
17	1	2.2	2.2	51	3	44.3	102.0
18	1	52.5	52.5	52	1	12.0	12.0
19	1	20.0	20.0	53	1	12.0	12.0
20	1	160.0	160.0	54	5	4.5	4.5
21	4	16.1	27.5	55	16	3.5	4.5
22	2	16.2	22.5	56	10	15.8	144.0
23	4	2.4	4.5	57	6	13.7	43.2
24	2	484.0	800.0	58	4	0.6	0.6
25	6	161.6	960.0	59	26	2.5	18
26	3	334.3	882.0	60	1	0.4	0.4
27	9	4.9	22.5	61	7	3.6	5.0
28	6	0.8	2.3	62	10	1.2	9.0
29	9	3.1	9.0	63	8	29.9	153.6
30	10	9.0	30.0	64	7	7.2	30.0
31	7	2.4	7.2	65	5	70.9	308.0
32	1	15.0	15.0	66	3	5.8	10.0
33	1	21.0	21.0	67	8	6.5	15.0
34	1	15.0	15.0	68	8	5.1	14.0

#### 4.3.3. Morphometric Characterization of the Accumulation and Detachment Areas

The accumulation area of the Pretare-Piedilama clastic deposits is characterized by an elongated shape (Figure 14a). The main morphometric parameters are shown in Figure 14b. The extent of the rock avalanche deposits is 1.98 km<sup>2</sup> with a run-out of more than 4 km from the source area to the southern edge (Figure 14c, section A-A'). In the proximal sector, from the source area to approximately the central part of the deposit (about 2 km), the clastic deposits are channelized with an elongation direction of NW-SE.

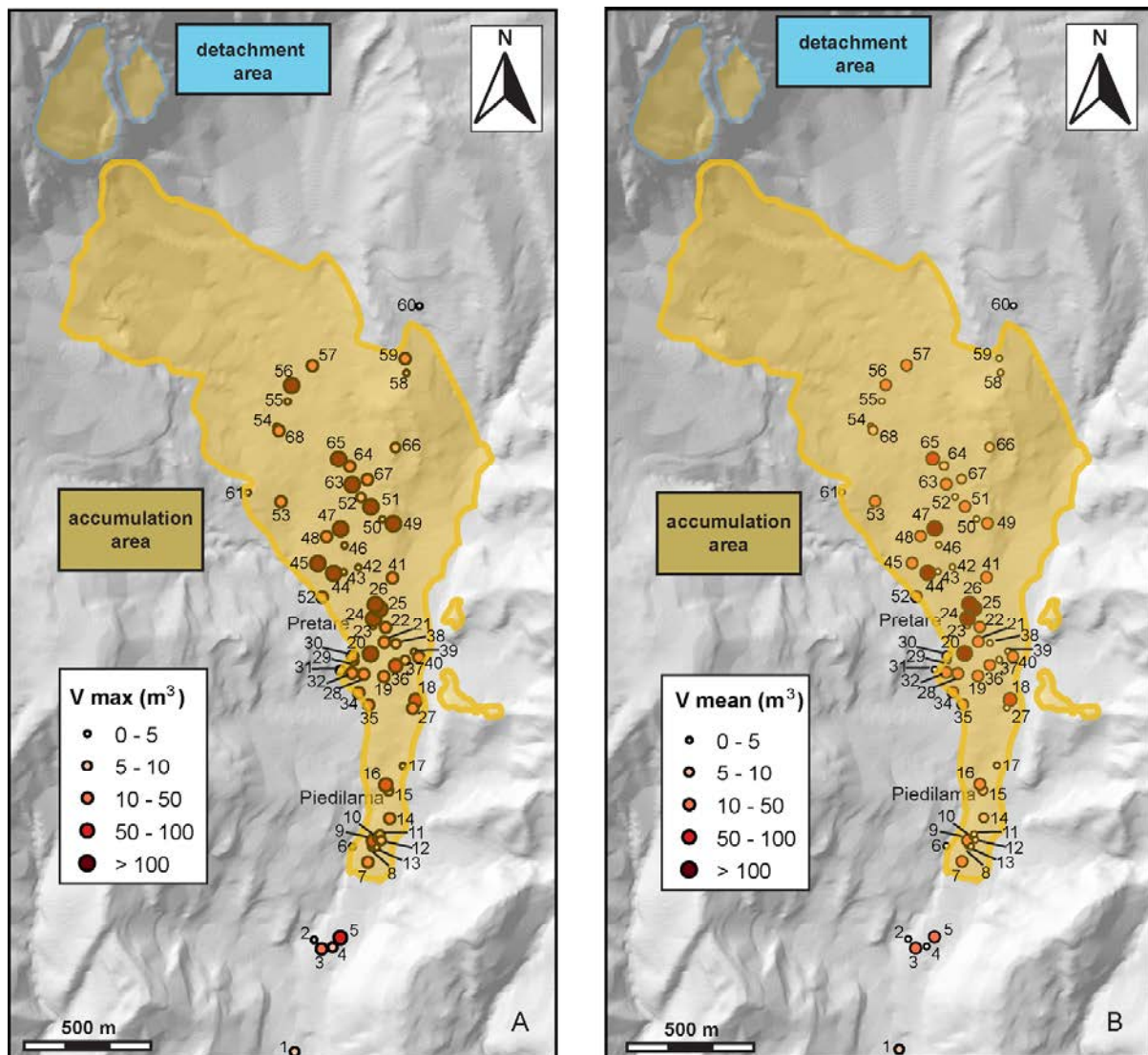


**Figure 13.** Spatial distribution of (A) maximum ( $V_{max}$ ) and (B) mean ( $V_{mean}$ ) block volume across the rock avalanche deposit. Each number refers to the corresponding station reported in Table 1.

In the down valley, the deposit spreads on an E-W axis and reaches the maximum planimetric width ( $W_a$ , approximately 1.2 km); here, the topographic surfaces of the landslide body end up deeply incised and bordered by a bedrock salient on its eastern edge (Figure 14d, section B-B'). The clastic deposits in the central and distal sectors are narrow and elongated in a N-S direction (Figure 14a) following the valley orientation. In several parts (e.g., Figure 14e, section C-C') a hummocky morphology can be noticed, which represents a typical feature of rock-avalanche deposits. As already observed in central Apennines for the Campo di Giove [24] and Lettopalena [25] rock avalanches, another typical feature of this kind of deposit is the presence of run-up zones, where the high-energy clastic flow can move counter-slope. In this case, two small clastic deposits were recognized overlying the arenaceous bedrock on the eastern slope of the Pretare-Piedilama Valley, (Figure 14f, section D-D'). The flowing mass could have had enough kinetic energy to climb up on the side of the valley. Nonetheless, it is important to note that the elevation difference between the valley floor and the run-up areas (approximately 50 m) is too high for assuming a simple run-up process. According to Tortorici et al. (2019) [58] the entire elevation difference was generated by the activity of a Quaternary west-dipping normal fault, the Pretare-Piedilama Fault, located at the base of the slope (Figures 5 and 14f).



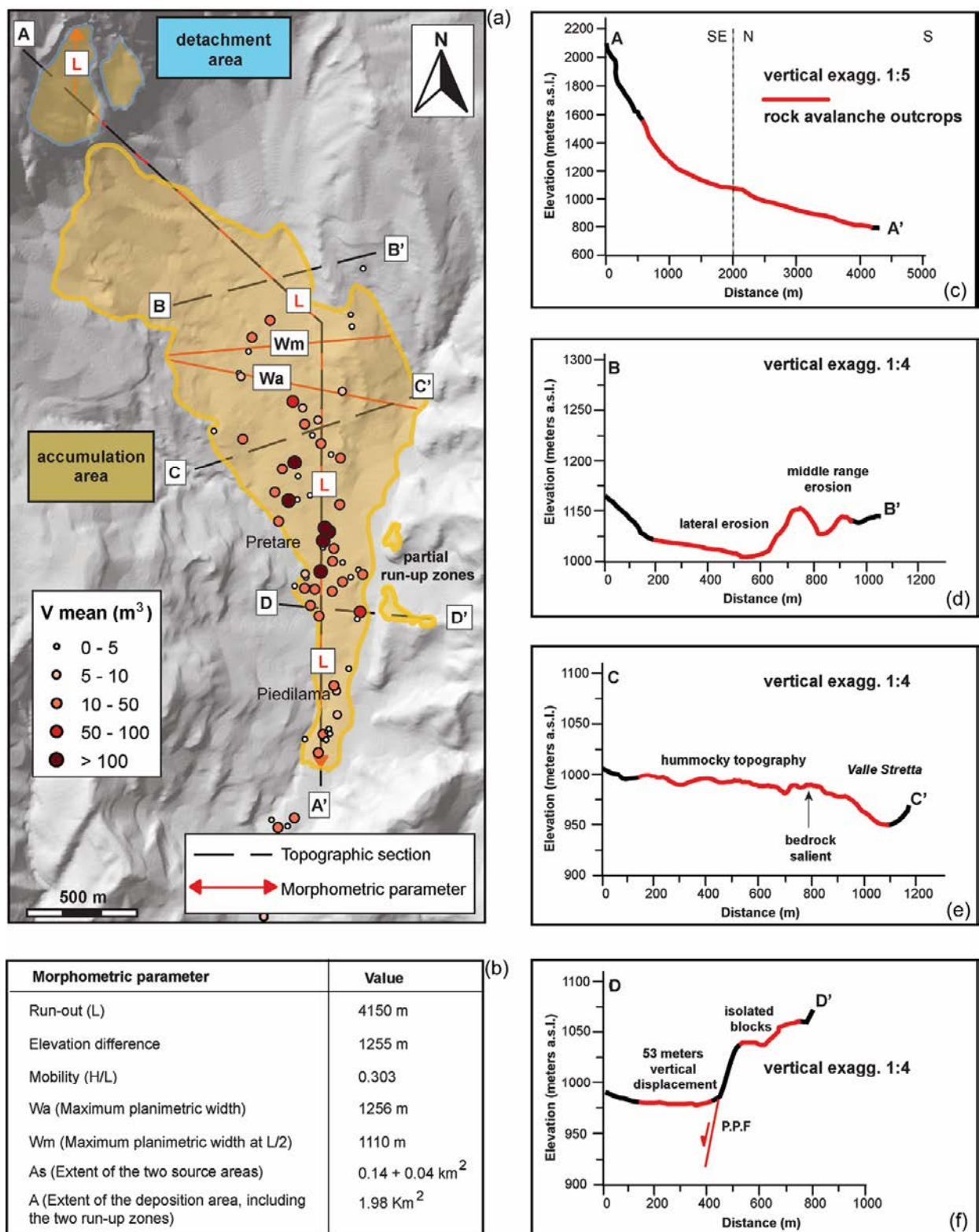


**Figure 14.** (a) Accumulation area of the Pretare-Piedilama rock avalanche ( $V_{mean}$  distribution is also reported); (b) main morphometric parameters; (c–f) topographic cross sections. Legend: P.P.F. = Pretare-Piedilama Fault.

The Pretare-Piedilama deposits originated from the south-eastern slope of the Sibillini Range where two box-shaped source areas can be clearly identified in the Aia della Regina area (Figure 12e). The detachment surface dips about  $30^\circ$  southeastward and presents

a staircase profile with three main steps (I–III in Figure 12f). A 2m-resolution DEM was used to outline the present topography (Figure 15a). The, pre- and post-failure DEM surfaces were compared for both detachment sub-areas, and a missing rock volume of about  $8.41 \times 10^6 \text{ m}^3$  was estimated. Therefore, a rough estimation of the volume in the accumulation area of the PRA deposit, based on the analysis of the boreholes and of the thicknesses observed in the field, is about  $10,56 \times 10^6 \text{ m}^3$ , which is comparable to the volume of the detachment mass calculated in the Aia della Regina area. The volume is increased by only about 25.6%, thus consequently it is assumed that there was limited expansion of the rock mass during the emplacement of the rock avalanche.

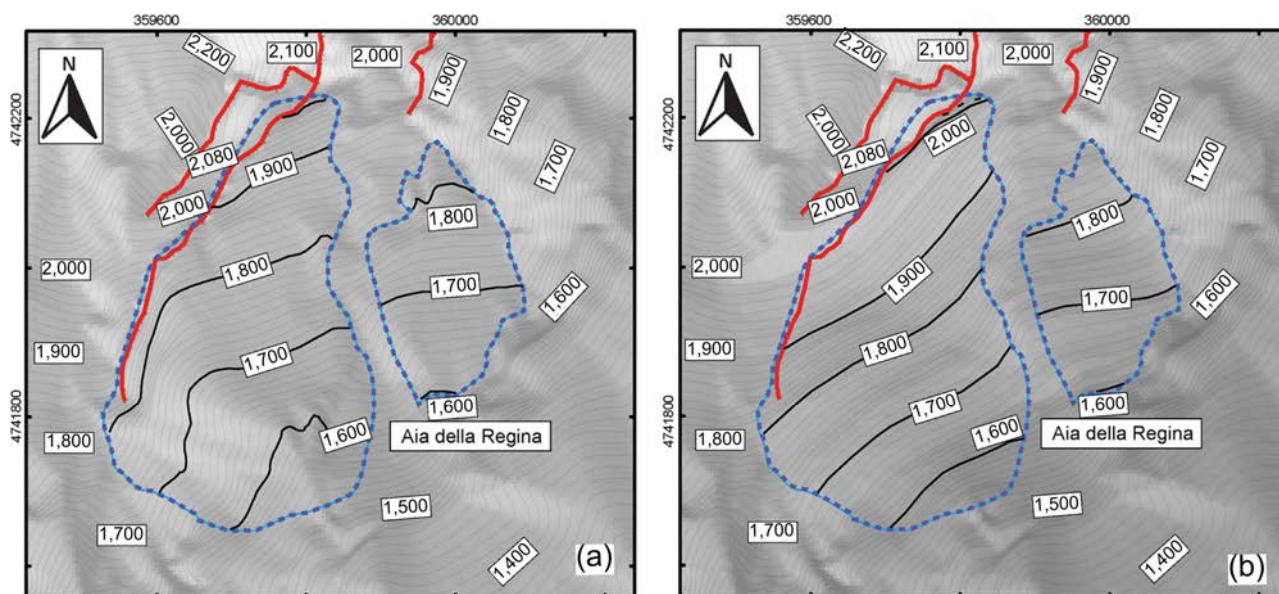


**Figure 15.** Aia della Regina source areas: 2D reconstruction of present-day (a) and pre-failure topography (b). Dashed, blue lines envelop detachment areas; the present escarpment is also traced. The projected coordinate system is UTM33N-WGS84.

## 5. Discussion and Conceptual Model

Much evidence described in this work that is based on geological and geomorphological field observations and measures are useful to describe the clastic deposits and to frame their origin within the Quaternary events affecting the investigated area.

The Pretare rock debris deposits are located in the south-eastern piedmont slope of Mt. Vettore, forming the infill deposits of the narrow Pretare-Piedilama fluvial valley. The arrangement of the Vettore mountain ridge in the hanging-wall and the folded Miocene siliciclastic in the footwall of the main thrust was responsible for the evolution of the Morriconne Stream valley. The results of the performed analyses shows a whole body thickness of the Quaternary sediments of about 74 m. The uppermost unit in Figure 4 corresponds to the outcrop of the PRA deposit. The well-log analysis has revealed the Quaternary landslide deposits placed at different depths, between the Miocene arenaceous bedrock and the PRA deposit. This means that the Pretare-Piedilama rock slope failure was framed within a continental environment whose evolution was characterized by high-energy depositional episodes alternating with low-energy stages (identified by fluvial plain clayey-silty deposits).

The PRA deposit is about 15 m thick, as recognized in boreholes, and the underlying unit 3 (Figures 3 and 5) is extensively located at the base of the M.te Vettore mountain slope. The PRA deposit was directly sourced by the slope of the Aia della Regina and retains the original stratigraphy in the detachment area, with a normal polarity. The main part of the debris is composed of clastic material of the Calcare Massiccio Fm (massive, shallow-water carbonates), while in the uppermost part of the accumulation area, blocks made by Corniola

Fm (thin-bedded micritic limestone) were observed. The basal part of the PRA shown in the borehole is characterized by a few meters of mixed carbonate and sandstones blocks. The latter deposit testifies to the the bedrock erosion made on siliciclastic rocks of the Laga Fm that generated the rock debris. Alluvial deposits are also found in the bottom sector of the borehole succession, evidencing the Morricone palaeostream which was covered by the detrital debris deposits.

In the sedimentary sequence found below the PRA deposit, the carbonate blocks are various in composition, and sandstone blocks and clasts are more frequent, highlighting a significant contribution coming from the sandstone slopes bounding the lateral valley. The PRA deposits are reworked in the lower part of the valley where terraced alluvial successions can be identified (unit 5 in Figure 5), and the Holocene deposits of the alluvial plain and valley floor (unit 6 in Figure 5) dissect the PRA and partially cover it.

The PRA clastic deposits forming the rock avalanche lie uncomfortably on the cross-cut Middle Pleistocene erosion surface [81] placed at about 1050 m of altitude a.s.l. representing the post-*quem* age of the deposition. According to Tortorici et al. (2009), Aringoli et al. (2014), and ISPRA 2021 [58,66,87,88], the age of the PRA deposits is Late Pleistocene and the depositional process was strictly connected to the cold climate events of the Late Pleistocene. As known in the literature, the cold climate was responsible for the deposition of fluvial sediments such as the younger fluvial deposits overlying the PRA deposit. A cut-and-fill process was the mechanism that was able to generate the fluvial terraces that could be hypothetically be assigned to post Late Pleistocene times.

The presence of isolated blocks within the main body of the PRA and north to Piedilama village (see Figure 14) is congruent with a vertical displacement of 53 m, which could be related to the presence of minor structures (named P.P.F.: Pretare-Piedilama fault in Figure 14). However, it cannot be excluded that the elevation of clastic deposits found on the opposite side of the valley were partly generated by a run-up of the rock avalanche during its emplacement against the uplifted flank of the bedrock.

The rock debris deposits filling the upper part of the Pretare-Piedilama valley can be interpreted as the remnant of more than one rock avalanche event developed after a massive rock slope failure from the eastern edge of the Sibillini Ridge during the Late Pleistocene. Such a hypothesis is supported by the sedimentary characteristics of the clastic sequence and by the morphometric setting of the accumulation area.

The sedimentological features are consistent with a high-energy transport and deposition and a dry granular flow. The deposit is composed of angular clasts and boulders ranging from few to hundreds  $m^3$ . Rock debris contains a sandy-gravel matrix, indicating an intense shattering mechanism of the rock mass. The presence of “carapace” facies and the preservation of the original slope stratigraphy (with normal polarity) are further clues which suggest the rock avalanche origin. Such evidence rules out the possible origin of the clastic material as a debris flow, as already proposed by Tortorici et al., (2009) [58].

The failure mechanism can be hypothesized as a planar sliding of about  $8,41 \cdot 10^6 m^3$  of rock material detached from a main, box-shaped detachment area. The asymmetric distribution of the debris accumulation area—with a NW-SE-oriented sector in the proximal part and a N-S narrowed concentration in the central and distal areas—was likely determined by an articulated morphology of the arenaceous/pelitic bedrock. Moreover, the reduced width of the valley prevented the radial spreading and forced the channelization of the rock flow. Down to the Pretare village, the valley’s narrowing to less than 300 m can explain the elevated number of blocks, even of great dimensions, which stopped in a small area (Figure 13A,B). Therefore, a rough estimation of the volume of the accumulation area of the PRA deposit, based on the analysis of the boreholes and of the thicknesses, was observed in the field and is of about about  $10,563 \times 10^6 m^3$ , which is comparable to the volume of the detachment mass calculated in the Aia della Regina area. The volume only increased by about 20.4%. Consequently, a limited expansion of the rock mass during the emplacement of the rock avalanche has been proposed.

Finally, residual geological hazards should be evaluated in terms of the possible seismically-induced reactivation of the landslide body. However, the 2016 central Italy earthquakes did not cause the palaeolandslide reactivation, while newly-generated, small-sized rock fall events occurred during the seismic sequence on the eastern edge of the Sibillini ridge around the rock avalanche detachment area. Thus, further studies should investigate the post-failure conditions of the rock slope to determine the possible presence of slope-scale gravitational processes.

## 6. Final Remarks

The present work concerns a multidisciplinary analysis integrating geological and geomorphological investigations and sedimentological, stratigraphic and morphometric analyses aimed at unravelling the origin of the Pretare rock debris deposits (PRA). Such deposits show a complex stratigraphic organization and their arrangement and geometry allowed us to interpret them as rock avalanches rather than debris flow deposits, as previously suggested. Furthermore, the PRA deposits were probably generated in a cold stadial climate of the Late Pleistocene.

The passive control of the fold-and-fault structures on the morphological development of the Morricone valley was outlined by many structural landforms, as shown in Figure 4. Furthermore, the morphometry of the Pretare rock avalanche deposit revealed a comparison between the rock deposit volume involved in the mass movement and that loss in the source area. The boulders in the Morricone valley are extremely variable in shape; in fact the largest boulders are found in the upper and central sector of the accumulation area, and a high number of blocks of different shapes are in the narrowing of the valley located south of the Pretare village (Figure 13A,B). Finally, the younger fluvial processes reworking the Pretare deposit and filling the Morricone valley are related to the most recent tectonic uplift of the Mt. Vettore area that triggered the vertical incision of the rivers, thus producing the fluvial terraces. In this paper we tried to make a contribution to the knowledge of the rock avalanche process, highlighting the role played by the geological structures and morphology in the activation and development processes.

**Author Contributions:** Conceptualization, M.L.P., E.D.L., L.S., A.P. and S.I.G.; methodology, M.L.P., E.D.L., L.S., A.P. and S.I.G.; software, E.D.L., L.S. and A.P.; validation, E.D.L., L.S. and A.P.; formal analysis, M.L.P., E.D.L., L.S., A.P. and S.I.G.; investigation, M.L.P., E.D.L. and L.S.; resources, M.L.P., E.D.L., L.S., A.P. and S.I.G.; data curation, M.L.P., E.D.L., L.S., A.P. and S.I.G.; writing—original draft preparation, M.L.P., E.D.L., L.S., A.P. and S.I.G.; writing—review and editing, M.L.P., E.D.L., L.S., A.P. and S.I.G.; visualization, M.L.P., E.D.L., L.S., A.P. and S.I.G.; supervision, M.L.P., E.D.L. and S.I.G. All authors have read and agreed to the published version of the manuscript.

**Funding:** This research received no external funding.

**Data Availability Statement:** Not applicable.

**Acknowledgments:** We wish to thank you for the critical reviews which improved the manuscript readability.

**Conflicts of Interest:** The authors declare that they have no conflict of interest.

## References

1. Hutchinson, J.N. General report: Morphological and geotechnical parameters of landslides in relation to geology and hydrogeology. In Proceedings of the 5th International Symposium on Landslides, Lausanne, Switzerland, 10–15 July 1988; pp. 3–35.
2. Hungr, O.; Evans, S.G. Entrainment of debris in rock avalanches: An analysis of a long runout-out mechanism. *Geol. Soc. Am. Bull.* **2004**, *116*, 1240–1252. [[CrossRef](#)]
3. Hungr, O.; Leroueil, S.; Picarelli, L. The Varnes classification of landslide types, an update. *Landslides* **2014**, *11*, 167–194. [[CrossRef](#)]
4. Hermanns, R.L.; Niedermann, S.; Garcia, A.V.; Schellenberger, A. Rock avalanching in the NW Argentine Andes as a result of complex interactions of lithologic, structural and topographic boundary conditions, climate change and active tectonics. In *Landslides from Massive Rock Slope Failure*; Evans, S.G., Scarascia Mugnozza, G., Strom, A.L., Hermanns, R.L., Eds.; Nato Science Series Book IV Earth and Environmental Sciences 49; Springer Publisher: Dordrecht, The Netherlands, 2006; pp. 497–520.
5. Mitchell, W.A.; Mc Saveney, M.J.; Zondervan, A.; Kim, K.; Dunning, S.A.; Taylor, P.J. The Keylong Serai rock avalanche, NW Indian Himalaya: Geomorphology and palaeoseismic implications. *Landslides* **2007**, *4*, 245–254. [[CrossRef](#)]

6. Penna, I.M.; Hermanns, R.L.; Niedermann, S.; Folgueral, A. Multiple slope failures associated with neotectonic activity in the Southern Central Andes (37°–37°30' S), Patagonia, Argentina. *Bull. Geol. Soc. Am.* **2011**, *123*, 1880–1895. [[CrossRef](#)]
7. Pánek, T.; Lenart, J.; Hradecký, J.; Hercman, H.; Braucher, R.; Šilhán, K.; Škarpich, V. Coastal cliffs, rock-slope failures and Late Quaternary transgressions of the Black Sea along southern Crimea. *Quat. Sci. Rev.* **2018**, *181*, 76–92. [[CrossRef](#)]
8. Delchiaro, M.; Della Seta, M.; Martino, S.; Dehbozorgi, M.; Nozaem, R. Reconstruction of river valley evolution before and after the emplacement of the giant Seymareh rock avalanche (Zagros Mts., Iran). *Earth Surf. Dyn.* **2019**, *7*, 929–947. [[CrossRef](#)]
9. Chigira, M.; Kiho, K. Deep-seated rockslide-avalanches preceded by mass rock creep of sedimentary rocks in the Akaishi Mountains, central Japan. *Eng. Geol.* **1994**, *38*, 221–230. [[CrossRef](#)]
10. Jain, S.K.; Nanda, A. A constitutive model for creep rupture. *Mech. Adv. Mater. Struct.* **2010**, *17*, 459–466. [[CrossRef](#)]
11. Pedrazzini, A.; Jaboyedoff, M.; Loye, A.; Derron, M.H. From deep seated slope deformation to rock avalanche: Destabilization and transportation models of the Sierre landslide (Switzerland). *Tectonophysics* **2013**, *605*, 149–168. [[CrossRef](#)]
12. Di Luzio, E.; Bianchi Fasani, G.; Saroli, M.; Esposito, C.; Cavinato, G.P.; Scarascia Mugnozza, G. Massive rock slope failure in the Central Apennines (Italy): The case of the Campo di Giove rock avalanche. *Bull. Eng. Geol. Environ.* **2004**, *63*, 1–12. [[CrossRef](#)]
13. Bianchi Fasani, G.; Di Luzio, E.; Esposito, C.; Evans, S.G.; Scarascia Mugnozza, G. Quaternary, catastrophic rock avalanches in the Central Apennines (Italy): Relationships with inherited tectonic features, gravity-driven deformations and the geodynamic frame. *Geomorphology* **2014**, *211*, 22–42. [[CrossRef](#)]
14. Esposito, C.; Di Luzio, E.; Scarascia Mugnozza, G.; Bianchi Fasani, G. Mutual interactions between slope-scale gravitational processes and morpho-structural evolution of central Apennines (Italy): Review of some selected case histories. *Rend. Lincei. Sci. Fis. E Nat.* **2014**, *25*, 151–165. [[CrossRef](#)]
15. Ostermann, M.; Sanders, D. The Benner pass rock avalanche cluster suggests a close relation between long-term slope deformation (DSGSDs and translational rock slides) and catastrophic failure. *Geomorphology* **2017**, *289*, 44–59. [[CrossRef](#)]
16. Glueer, F.; Loew, S.; Manconi, A.; Aaron, J. From toppling to sliding: Progressive evolution of the Moosfluh Landslide, Switzerland. *J. Geophys. Res. Earth Surf.* **2019**, *124*, 2899–2919. [[CrossRef](#)]
17. Semenza, E.; Ghirotti, M. History of the 1963 Vajont slide: The importance of geological factors. *Bull. Eng. Geol. Environ.* **2000**, *59*, 87–97. [[CrossRef](#)]
18. Genevois, R.; Ghirotti, M. The 1963 Vaiont landslide. *G. Geol. Appl.* **2005**, *1*, 41–52. [[CrossRef](#)]
19. Dramis, F.; Govi, M.; Guglielmin, M.; Mortara, G. Mountain permafrost and slope instability in the Italian Alps: The Val Pola landslide. *Permafr. Periglac. Process.* **1995**, *6*, 73–81. [[CrossRef](#)]
20. Crosta, G.B.; Chen, H.; Lee, C.F. Replay of the 1987 Val Pola Landslide, Italian Alps. *Geomorphology* **2004**, *60*, 127–146. [[CrossRef](#)]
21. Nicoletti, P.G.; Parise, M.; Miccadei, E. The Scanno rock avalanche (Abruzzi, south-central Italy). *Boll. Soc. Geol. Ital.* **1993**, *112*, 523–525.
22. Cinti, G.; Donati, A.; Scarascia Mugnozza, G. La grande frana di Monte Arezzo (Abruzzo). *Mem. Soc. Geol. Ital.* **2001**, *56*, 41–50.
23. Paolucci, G.; Pizzi, R.; Scarascia Mugnozza, G. Analisi preliminare della frana di Lettopalena (Abruzzo). *Mem. Soc. Geol. Ital.* **2001**, *56*, 131–137.
24. Giano, S.I.; Schiattarella, M. Drainage integration of small endorheic basins at the Pleistocene-Holocene transition: An example from southern Italy. *Geomorphology* **2023**, *427*, 108622. [[CrossRef](#)]
25. Scarascia Mugnozza, G.; Bianchi Fasani, G.; Esposito, C.; Martino, S.; Saroli, M.; Di Luzio, E.; Evans, S.G. Rock avalanche and mountain slope deformation in a convex, dipslope: The case of the Majella massif (Central Italy). In *Landslides from Massive Rock Slope Failure*; Evans, S.G., Scarascia Mugnozza, G., Strom, A.L., Hermanns, R.L., Eds.; Nato Science Series Book IV Earth and Environmental Sciences 49; Springer Publisher: Dordrecht, The Netherlands, 2006; pp. 357–376.
26. Della Seta, M.; Esposito, C.; Marmoni, G.M.; Martino, S.; Scarascia Mugnozza, G.; Troiani, F. Morpho-structural evolution of the valley-slope systems and related implications on slope-scale gravitational processes: New results from the Mt. Genzana case history (Central Apennines, Italy). *Geomorphology* **2017**, *289*, 60–77. [[CrossRef](#)]
27. Antonielli, B.; Della Seta, M.; Esposito, C.; Scarascia Mugnozza, G.; Schilirò, L.; Spadi, M.; Tallini, M. Quaternary rock avalanches in the Apennines: New data and interpretation of the huge clastic deposit of the L'Aquila Basin (central Italy). *Geomorphology* **2020**, *361*, 107194. [[CrossRef](#)]
28. McSaveney, M.J.; Davies, T.R.H. Rapid rock mass flow with dynamic fragmentation: Inferences from the morphology and internal structure of rockslides and rock avalanches. In *Landslides from Massive Rock Slope Failure*; Evans, S.G., Scarascia Mugnozza, G., Strom, A.L., Hermanns, R.L., Eds.; Nato Science Series Book IV Earth and Environmental Sciences 49; Springer Publisher: Dordrecht, The Netherlands, 2006; pp. 285–304.
29. Owen, L.A.; Kamp, U.; Khattak, G.A.; Harp, E.L.; Keefer, D.K.; Bauer, M.A. Landslides triggered by the 8 October 2005 Kashmir earthquake. *Geomorphology* **2008**, *94*, 1–9. [[CrossRef](#)]
30. Hewitt, K. Rock avalanche dams on the Trans Himalayan Upper Indus streams: A survey of Late Quaternary events and hazard-related characteristics. In *Natural and Artificial Rockslide Dams*; Evans, S., Hermanns, R., Strom, A., Scarascia Mugnozza, G., Eds.; Lecture Notes in Earth Sciences 133; Springer: Berlin/Heidelberg, Germany, 2011; pp. 177–204. [[CrossRef](#)]
31. Ren, Z.; Wang, K.; Yang, K.; Zhou, Z.-H.; Tang, Y.-J.; Tian, L.; Xu, Z.-M. The grain size distribution and composition of the Touzhai rock avalanche deposit in Yunnan, China. *Eng. Geol.* **2018**, *234*, 97–111. [[CrossRef](#)]
32. Dunning, S.A. The grain size distribution of rock-avalanche deposits in valley confined settings. *Ital. J. Eng. Geol. Environ.* **2006**, *1*, 117–121. [[CrossRef](#)]

33. Schilirò, L.; Esposito, C.; De Blasio, F.V.; Scarascia Mugnozza, G. Sediment texture in rock avalanche deposits: Insights from field and experimental observations. *Landslides* **2019**, *16*, 1629–1643. [[CrossRef](#)]
34. Shugar, D.H.; Clague, J.J. The sedimentology and geomorphology of rock avalanche deposits on glaciers. *Sedimentology* **2011**, *58*, 1762–1783. [[CrossRef](#)]
35. Dunning, S.A.; Rosser, N.J.; McColl, S.T.; Reznichenko, N.V. Rapid sequestration of rock avalanche deposits within glaciers. *Nat. Commun.* **2015**, *6*, 7964. [[CrossRef](#)]
36. McColl, S.T.; Davies, T.R.H. Evidence for a rock-avalanche origin for ‘The Hillocks’ ‘moraine’, Otago, New Zealand. *Geomorphology* **2011**, *127*, 216–224. [[CrossRef](#)]
37. De Blasio, F.V.; Medici, L. Microscopic model of rock melting beneath landslides calibrated on the mineralogical analysis of the Köfels frictionite. *Landslides* **2016**, *14*, 337–350. [[CrossRef](#)]
38. Dufresne, A.; Geertsema, M.; Shugar, D.H.; Koppes, M.; Higman, B.; Haeussler, P.J.; Stark, C.; Venditti, J.G.; Bonno, D.; Larseni, C.; et al. Sedimentology and geomorphology of a large tsunamigenic landslide, Taan Fiord, Alaska. *Sediment. Geol.* **2018**, *364*, 302–318. [[CrossRef](#)]
39. Davies, T.; McSaveney, M.J. Runout of dry granular avalanches. *Can. Geotech. J.* **1999**, *36*, 313–320. [[CrossRef](#)]
40. Legros, F. Can dispersive pressure cause inverse grading in grain flows? *J. Sediment. Res.* **2002**, *72*, 166–170. [[CrossRef](#)]
41. Dufresne, A.; Davies, T.; McSaveney, M. Influence of runout-path material on emplacement of the Round Top rock avalanche, New Zealand. *Earth Surf. Process. Landf.* **2010**, *35*, 190–201. [[CrossRef](#)]
42. Aaron, J.; Wolter, A.; Loew, S.; Volken, S. Understanding Failure and Runout Mechanisms of the Flims Rockslide/Rock Avalanche. *Front. Earth Sci.* **2020**, *8*, 224. [[CrossRef](#)]
43. Mitchell, A.; McDougall, S.; Aaron, J.; Brideau, M.A. Rock Avalanche-Generated Sediment Mass Flows: Definitions and Hazard. *Front. Earth Sci.* **2020**, *8*, 543937. [[CrossRef](#)]
44. Davies, T.; McSaveney, M.J.; Hodgson, K.A. A fragmentation-spreading model for long runout rock avalanches. *Can. Geotech. J.* **1999**, *36*, 1096–1110. [[CrossRef](#)]
45. Evans, S.G.; Scarascia Mugnozza, G.; Strom, A.; Hermanns, R.L. Landslide from massive rock slope failure and associated phenomena. In *Landslides from Massive Rock Slope Failure*; Evans, S.G., Scarascia Mugnozza, G., Strom, A.L., Hermanns, R.L., Eds.; Nato Science Series Book IV Earth and Environmental Sciences; Springer Publisher: Dordrecht, The Netherlands, 2006; Volume 49, pp. 3–52.
46. Mangeney, A.; Roche, O.; Hungr, O.; Mangold, N.; Faccanoni, G.; Lucas, A. Erosion and mobility in granular collapse over sloping beds. *J. Geophys. Res. Earth Surf.* **2010**, *115*, F03040. [[CrossRef](#)]
47. Bowman, E.T.; Take, W.A.; Rait, K.L.; Hann, C. Physical models of rock avalanche spreading behaviour with dynamic fragmentation. *Can. Geotech. J.* **2012**, *49*, 460–476. [[CrossRef](#)]
48. Schleier, M.; Hermanns, R.L.; Rohn, J. Spatial distribution of rockslide deposits suggest timing and paleo-environmental conditions for rock slope failures in Innerdalen and Innfjorddalen, Møre og Romsdal county, western Norway. *Ital. J. Eng. Geol. Environ.* **2013**, *Book Series 6*, 493–505. [[CrossRef](#)]
49. Dufresne, A.; Dunning, S.A. Process dependence of grain size distributions in rock avalanche deposits. *Landslides* **2017**, *14*, 1555–1563. [[CrossRef](#)]
50. Orwin, J.F.; Clague, J.J.; Gerath, R.F. The Cheam rock avalanche, Fraser Valley, British Columbia, Canada. *Landslides* **2004**, *1*, 289–298. [[CrossRef](#)]
51. Strom, A.L.; Korup, O. Extremely large rockslides and rock avalanches in the Tien Shan Mountains, Kyrgyzstan. *Landslides* **2006**, *3*, 125–136. [[CrossRef](#)]
52. Dai, F.C.; Tu, X.B.; Xu, C.; Gong, Q.M.; Yao, X. Rock avalanches triggered by oblique thrusting during the 12 May 2008 Ms 8.0 Wenchuan earthquake, China. *Geomorphology* **2011**, *132*, 300–318. [[CrossRef](#)]
53. Bianchi Fasani, G. Grandi Frane in Roccia: Fenomenologia ed Evidenze di Terreno. Ph.D. Thesis, University of Rome ‘‘Sapienza’’, Rome, Italy, 2004; 192p.
54. Crosta, G.B.; Frattini, P.; Fusi, N. Fragmentation in the Val Pola rock avalanche. Italian Alps. *J. Geophys. Res.* **2007**, *112*, F01006. [[CrossRef](#)]
55. Knapp, S.; Krautblatter, M. Conceptual Framework of Energy Dissipation During Disintegration in Rock Avalanches. *Front. Earth Sci.* **2020**, *8*, 263. [[CrossRef](#)]
56. Vezzani, L.; Festa, A.; Ghisetti, F.C. *Geology and tectonic Evolution of the Central-Southern Apennines, Italy*; The Geological Society of America: Boulder, CO, USA, 2010; Volume 469. [[CrossRef](#)]
57. Pierantoni, P.; Deiana, G.; Galdenzi, S. Stratigraphic and structural features of the Sibillini Mountains (Umbria-Marche Apennines, Italy). *Ital. J. Geosci.* **2013**, *132*, 497–520. [[CrossRef](#)]
58. Tortorici, G.; Romagnoli, G.; Grassi, S.; Imposa, S.; Lombardo, G.; Panzera, F.; Catalano, S. Quaternary negative tectonic inversion along the Sibillini Mts. thrust zone: The Arquata del Tronto case history (Central Italy). *Environ. Earth Sci.* **2019**, *78*, 37. [[CrossRef](#)]
59. Galli, P.; Peronace, E.; Brammerini, F.; Castenetto, S.; Naso, G.; Cassone, F.; Pallone, F. The MCS intensity distribution of the devastating 24 August 2016 earthquake in central Italy (MW 6.2). *Ann. Geophys.* **2016**, *59*, 5. [[CrossRef](#)]
60. Rossi, A.; Tertulliani, A.; Azzaro, R.; Graziani, L.; Rovida, A.; Maramai, A.; Pessina, V.; Hailemichael, S.; Buffarini, G.; Bernardini, F.; et al. The 2016–2017 earthquake sequence in Central Italy: Macroseismic survey and damage scenario through the EMS-98 intensity assessment. *Bull. Earthq. Eng.* **2019**, *17*, 2407–2431. [[CrossRef](#)]

61. Luzi, L.; Pacor, F.; Lanzano, G.; Felicetta, C.; Puglia, R.; D'Amico, M. Central Italy seismic sequence: Strong motion data analysis and design earthquake selection for seismic microzonation purposes. *Bull. Earthq. Eng.* **2020**, *18*, 5533–5551. [[CrossRef](#)]
62. Regione Marche: Microzonazione Sismica. Available online: <https://qmap-protciv.regione.marche.it/cs/> (accessed on 18 May 2020).
63. Centamore, E.; Cantalamessa, G.; Micarelli, A.; Potetti, M.; Berti, D.; Bigi, S.; Morelli, C.; Ridolfi, M. Stratigrafia e analisi di facies dei depositi del Miocene e del Pliocene inferiore dell'avanfossa marchigiano-abruzzese e delle zone limitrofe. *Studi Geol. Camerti* **1991**, *2*, 125–131.
64. Milli, S.; Moscatelli, M.; Stanzione, O.; Falcini, F. Sedimentology and physical stratigraphy of the Messinian turbidite deposits of the Laga Basin (central Apennines, Italy). *Boll. Soc. Geol. Ital.* **2007**, *126*, 255–281.
65. Marini, M.; Felletti, F.; Milli, S.; Patacci, M. The thick-bedded tail of turbidite thickness distribution as a proxy for flow confinement: Examples from tertiary basins of central and northern Apennines (Italy). *Sediment. Geol.* **2016**, *341*, 96–118. [[CrossRef](#)]
66. ISPRA; Marino, M.; Muraro, C.; Papisodaro, F. Substrato Carbonatico e Depositi Quaternari Associati; M.L. Putignano, D. Domenico, M. Cesarano, M. Mancini: Substrato Silicoclastico e Depositi Quaternari Associate (a Cura di). "Note Illustrative Della Carta Geologica D'italia Alla Scala 1:50.000" F. 347 Norcia. 2021; p. 351. Available online: [https://www.isprambiente.gov.it/Media/carg/note\\_illustrative/337\\_Norcia.pdf](https://www.isprambiente.gov.it/Media/carg/note_illustrative/337_Norcia.pdf) (accessed on 10 February 2023).
67. ASTM D422-63; Standard Test Method for Particle-Size Analysis of Soils (Withdrawn 2016). ASTM International: West Conshohocken, PA, USA, 2007. [[CrossRef](#)]
68. Hutchinson, M.F.; Hoog, F. Smoothing Noisy Data with Spline Functions. *Numer. Math.* **1985**, *47*, 99–106. [[CrossRef](#)]
69. Hutchinson, M.F. Adding the Z-dimension. In *Handbook of Geographic Information Science*; Wilson, J.P., Fotheringham, A.S., Eds.; Blackwell: Oxford, UK, 2008; pp. 144–168.
70. Boccaletti, M.; Calamita, F.; Deiana, G.; Gelati, R.; Massari, F.; Moratti, G.; Ricci Lucchi, F. Migrating foredeep-thrust belt systems in the northern Apennines and southern Alps. *Palaeogeogr. Palaeoclimatol. Palaeoecol.* **1990**, *77*, 3–14. [[CrossRef](#)]
71. Patacca, E.; Sartori, R.; Scandone, P. Tyrrhenian Basin and Apenninic Arcs: Kinematic Relations since Late Tortonian Times. *Mem. Soc. Geol. Ital.* **1990**, *45*, 425–451.
72. Calamita, F.; Deiana, G. Correlazione tra gli eventi deformativi neogenico-quaternari del settore tosco-umbro-marchigiano. *Studi Geol. Camerti* **1995**, *1*, 137–152.
73. Ricci Lucchi, F. Miocene Paleogeography and basin analysis in the Periadriatic Apennines. In *Geology of Italy*; Squires, C., Ed.; Petroleum exploration society of Libya: Tripoli, Libya, 1975; pp. 5–111.
74. Cantalamessa, G.; Centamore, E.; Chiocchini, U.; Di Lorito, L.; Leonelli, M.; Micarelli, A.; Pesaresi, A.; Potetti, M.; Taddei, L.; Venanzini, D. (1980)—Analisi dell'evoluzione tettonico-sedimentaria dei "bacini minori" torbiditici del Miocene medio-superiore nell'Appennino umbro-marchigiano e laziale-abruzzese: 8) Il bacino della Laga tra il F. Fiastrone-T. Fiastrella ed il T. Fluvione. *Studi Geol. Camerti* **1980**, *6*, 81–133.
75. Koopman, A. Detachment tectonics in the central Apennines, Italy. *Geol. Ultraiectina* **1983**, *30*, 1–155.
76. Lavecchia, G. Il sovrascorrimento dei Monti Sibillini: Analisi strutturale e cinematica. *Boll. Soc. Geol. Ital.* **1985**, *104*, 161–194.
77. Turtù, A.; Satolli, S.; Maniscalco, R.; Calamita, F.; Speranza, F. Understanding progressive-arc- and strike-slip-related rotations in curve-shaped orogenic belts: The case of the Olevano-Antrodoco-Sibillini thrust (Northern Apennines, Italy). *J. Geophys. Res. Solid Earth* **2013**, *118*, 459–473. [[CrossRef](#)]
78. Di Domenica, A.; Bonini, L.; Calamita, F.; Toscani, G.; Galuppo, C.; Seno, S. Analogue modeling of positive inversion tectonics along differently oriented pre-thrusting normal faults: An application to the Central-Northern Apennines of Italy. *Geol. Soc. Am. Bull.* **2014**, *126*, 946–955. [[CrossRef](#)]
79. Galadini, F.; Galli, P. Active Tectonics in the Central Apennines (Italy)—Input Data for Seismic Hazard Assessment. *Nat. Hazards* **2000**, *22*, 225–268. [[CrossRef](#)]
80. Rovida, A.; Locati, M.; Camassi, R.; Lolli, B.; Gasperini, P. The Italian earthquake catalogue CPTI15. *Bull. Earthq. Eng.* **2020**, *18*, 2953–2984. [[CrossRef](#)]
81. Aringoli, D.; Cavitolo, P.; Farabollini, P.; Gentili, B.; Giano, S.; Lopez-Garrido, A.; Materazzi, M.; Nibbi, L.; Pedrera, A.; Pambianchi, G.; et al. Morphotectonic characterization of the quaternary intermontane basins in the Umbria-Marche Apennines (Italy). *Rend. Lincei Sci. Fis. Nat.* **2014**, *25* (Suppl. 2), 111–128. [[CrossRef](#)]
82. Pizzi, A.; Galadini, F. Pre-existing cross-structures and active fault segmentation in the Northern central Apennines. *Tectonophysics* **2009**, *476*, 302–319. [[CrossRef](#)]
83. Cacciuni, A.; Centamore, E.; Di Stefano, R.; Dramis, F. Evoluzione morfotettonica della conca di Amatrice. *Studi Geol. Camerti* **1995**, *2*, 95–100.
84. Sembroni, A.; Molin, P.; Soligo, M.; Tuccimei, P.; Anzalone, E.; Billi, A.; Franchini, S.; Ranaldi, M.; Tarchini, L. The uplift of the Adriatic flank of the Apennines since Middle Pleistocene: New insights from the Tronto River basin and the Acquasanta Terme Travertine (central Italy). *Geomorphology* **2019**, *352*, 106990. [[CrossRef](#)]
85. Coltorti, M.; Pieruccini, P. The planation surface across the Italian peninsula: A key tool in neotectonics studies. *J. Geodyn.* **2000**, *29*, 323–328. [[CrossRef](#)]
86. Dramis, F.; Pambianchi, G.; Nesci, O.; Consoli, M. Il ruolo di elementi strutturali trasversali nell'evoluzione tettonico-sedimentaria e geomorfologica della regione marchigiana. *Studi Geol. Camerti* **1991**, *2*, 287–293.

87. Aringoli, D.; Farabollini, P.; Pambianchi, G.; Materazzi, M.; Bufalini, M.; Fuffa, E.; Gentilucci, M.; Scalella, G. Geomorphological Hazard in Active Tectonics Area: Study Cases from Sibillini Mountains Thrust System (Central Apennines). *Land* **2021**, *10*, 510. [[CrossRef](#)]
88. Cesarano, M.; Putignano, M.L. Tettonica Compressiva e Distensiva Post-Orogenica Del Bacino Della Laga. In: M. Marino, C., Muraro, F. Papasodaro: Substrato Carbonatico e Depositi Quaternari Associati; M.L. Putignano, D. Domenico, M. Cesarano, M. Mancini: Substrato Silicoclastico e Depositi Quaternari Associate (a cura di). "Note Illustrative Della Carta Geologica d'Italia alla scala 1:50.000" F. 347 Norcia; 2021; pp. 221–232. Available online: [https://www.isprambiente.gov.it/Media/carg/note\\_illustrative/337\\_Norcia.pdf](https://www.isprambiente.gov.it/Media/carg/note_illustrative/337_Norcia.pdf) (accessed on 10 February 2023).

**Disclaimer/Publisher's Note:** The statements, opinions and data contained in all publications are solely those of the individual author(s) and contributor(s) and not of MDPI and/or the editor(s). MDPI and/or the editor(s) disclaim responsibility for any injury to people or property resulting from any ideas, methods, instructions or products referred to in the content.